



Curtin University

Centre for Marine Science and Technology

*Ship Motion Measurements
for
Ship Under-Keel Clearance
in the Port of Geraldton*

Prepared for:
Mid West Ports Authority



Prepared by: Jeong Hun Ha and Tim Gourlay

CMST Report: 2016-28

Date: 6th December 2016

SUMMARY

This report presents some results from a set of recent full-scale trials measuring dynamic sinkage, trim and heel of eleven bulk carrier transits entering and leaving the Port of Geraldton. Measurements were carried out using high-accuracy GNSS receivers and a fixed reference station. Measured sinkage, together with ship speed and channel bathymetry, are shown. Maximum dynamic sinkage and dynamic draught, as well as elevations of the ship's keel relative to Chart Datum are also shown. Additional comparisons of dynamic trim and heel between the transits are given.

Results from three of the transits, together with validation of ship squat modelling, have been published in an international conference paper. This is included in Appendix F. In future work, the measured results will be used for validating wave-induced motions software.



TABLE OF CONTENTS

	Page
SUMMARY	1
1. DETAILS OF SHIP MOTION TRIALS.....	3
1.1. Ships and measurement dates	3
1.2. Ship motion measurement equipment	3
1.3. Description of the procedure	5
2. ENVIRONMENTAL DATA	6
3. BATHYMETRIC DATA	7
4. DATA PROCESSING	7
5. RESULTS	8
5.1. Measured ship tracks	8
5.2. Individual measurement results	8
5.3. Comparisons between the transits	11
Appendix A – Details of the ships and transit conditions	
Appendix B – Tidal and wave (sea/swell) data	
Appendix C – Measured ship tracks	
Appendix D – Measured dynamic sinkage and UKC (Graphical results)	
Appendix E – Measured dynamic trim and heel (Graphical results)	
Appendix F – Published paper	

1. DETAILS OF SHIP MOTION TRIALS

In September and October 2015, at the Port of Geraldton, full-scale trials were performed on 11 inbound and outbound bulk carrier transits via its curved approach channel (see chart AUS81). The purpose of the trials is not only to obtain high-quality data on vertical ship motions in the port approach channel including squat and wave-induced motions, but also to validate current Under-Keel Clearance (UKC) practice using the data from the measurements.

1.1. Ships and measurement dates

Measurements were made on 11 bulk carrier transits, on the following dates:

- ▶ 1st set of measurements (31st August 2015 ~ 3rd September 2015, 4 days)
 - HONG YUAN, inbound, Wed 2nd September 2015
 - PETANI, inbound, Thu 3rd September 2015
 - DONNACONA, inbound, Thu 3rd September 2015
- ▶ 2nd set of measurements (27th September 2015 ~ 2nd October 2015, 6 days)
 - GUO DIAN 17, outbound, Mon 28th September 2015
 - SFL SPEY, outbound, Mon 28th September 2015
 - AAL FREMANTLE, inbound, Mon 28th September 2015
 - IVS MAGPIE, outbound, Mon 28th September 2015
 - FENG HUANG FENG, outbound, Tue 29th September 2015
 - AAL FREMANTLE, outbound, Wed 30th September 2015
 - SEA DIAMOND, inbound, Thu 1st October 2015
 - SEA DIAMOND, outbound, Fri 2nd October 2015

Ship dimensions and comparative transit conditions for all the ships are shown in Appendix A.

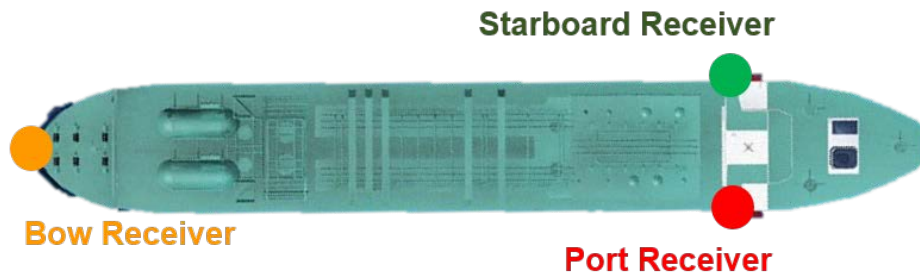
1.2. Ship motion measurement equipment

Ship motions were measured using Sokkia GSR2700 ISX and Trimble R10 GNSS receivers for the first and second set of measurements respectively. Four receivers were used for each set of measurements, with one in each of the following locations:

- Base station fixed to pilot jetty
- Roving receiver fixed to ship bow
- Roving receiver fixed to port bridge wing
- Roving receiver fixed to starboard bridge wing

An example GNSS equipment setup at the Port of Geraldton is shown in Figure 1.

(a)



(b)



(c)



(d)



(e)



Figure 1. GNSS receivers setup. (a) Plan view of ship receivers. (b) Base station on pilot jetty in the AAL FREMANTLE (inbound) transit. (c) Bow receiver in the SEA DIAMOND (outbound) transit. (d) Port receiver on bridge wing in the GUO DIAN 17 (outbound) transit. (e) Starboard receiver on bridge wing in the GUO DIAN 17 (outbound) transit.

With reference to Figure 1 (b), the base station was placed at two points on the pilot jetty for each set of trials, as shown in Figure 2. A blue point ($28^{\circ} 46' 33.31''$ S, $114^{\circ} 36' 8.03''$ E) is the base station location for the first set of trials, and a red point ($28^{\circ} 46' 33.26''$ S, $114^{\circ} 36' 6.34''$ E) is for the second set of trials. During the first set of trials, since Sokkia GSR2700 receivers have a power input, we set up the base station at the blue point where power supply is available, just in case. However, Trimble R10 receivers for the second set of trials do not have a power input, and hence the base station was moved to the red point for being in a more open area.



Figure 2. Base station location on pilot jetty.

1.3. Description of the procedure

The procedure for inbound transits is:

- CMST researchers board vessel with pilot
- Set up GNSS receivers on bow and both port and starboard bridge wings (symmetric positions)
- Data recording throughout pilotage
- Remove equipment and disembark with pilot

The procedure for outbound transits is the reverse of the above. Data recording covers a period of time before departure or after arrival to take a stationary reading at the berth. In our trials, data recording was commenced prior to leaving the berth for the outbound transits and continued until after all mooring work had been completed for the inbound transits. The at-berth measurements were then used as a reference value for comparing the vertical height measurements while under way.

2. ENVIRONMENTAL DATA

Tidal data that is raw sea surface elevations as measured at Berth 3-4 ($28^{\circ} 46' 36''$ S, $114^{\circ} 35' 46''$ E) in the Port of Geraldton has been provided by Mid West Ports Authority (hereafter referred to as MWPA). Independent local tide for each transit has been extracted from the raw sea surface data using a low-pass filter with a cutoff period of 5 minutes, and then applied to calculate dynamic sinkage of the ships. The tidal data covering the period of our measurements is shown in Appendix B.

Regarding wave data, some of the wave data from the AWAC (Acoustic Wave And Current Profiler) at Beacon 2 ($28^{\circ} 45' 28.2''$ S, $114^{\circ} 33' 55.9''$ E), located at the end of the channel, have also been provided by MWPA, shown in Appendix B. Wave heights and periods are presented as the sea and swell components, and sea/swell cutoff is 8 seconds.

During the trials, waves were measured by the AWAC at Beacon 2 and also by 10 pressure sensors at all the starboard hand beacons, i.e. Beacon 1, Beacon 3, Beacon 5, ..., Beacon 19, shown as red circles in Figure 3. The full measured wave time-series data will be used to study wave-induced motions in the channel, in future work.

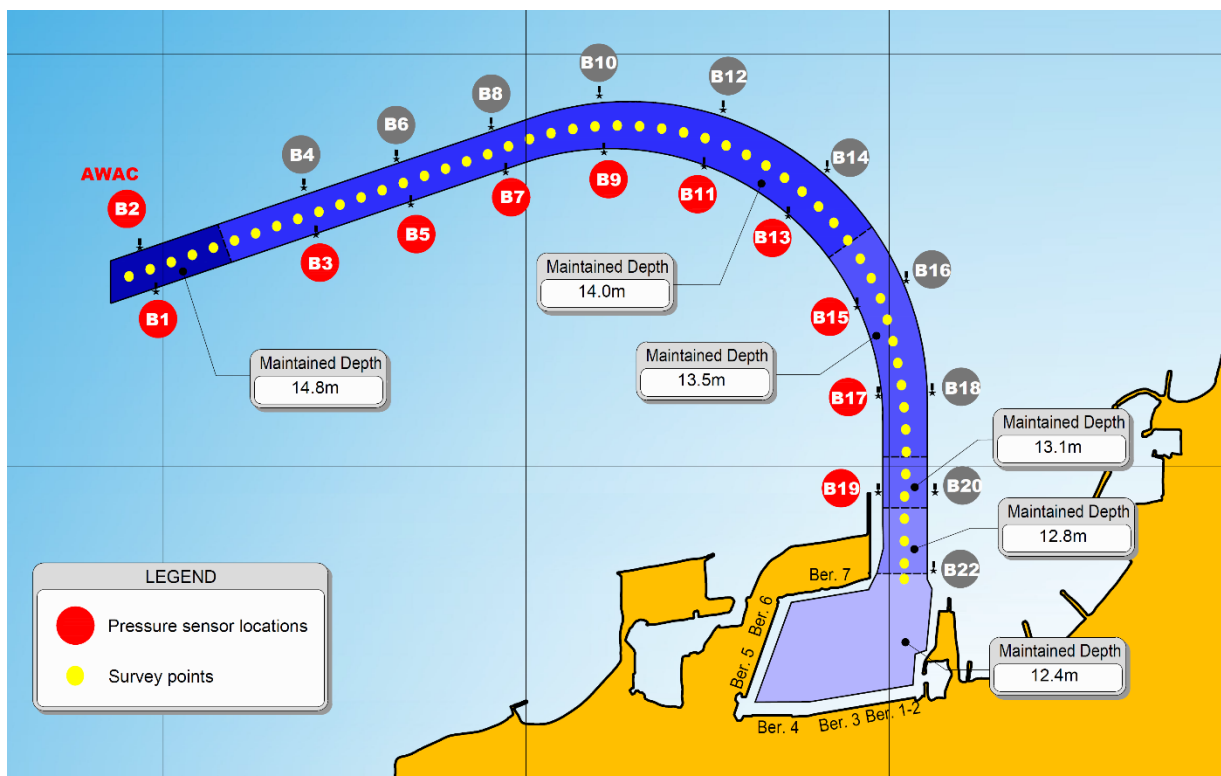


Figure 3. Wave pressure sensor locations and actual survey points in the channel.

3. BATHYMETRIC DATA

To give the keel heights relative to the seabed, we have used 53 survey points for the channel as provided by OMC International, shown as yellow points in Figure 3. A comparison between the bathymetry based on chart AUS81 and the survey points is shown in Figure 4. A flat seabed line is based on the charted depth on AUS81, and a fluctuating seabed line is the actual survey line provided by OMC International.

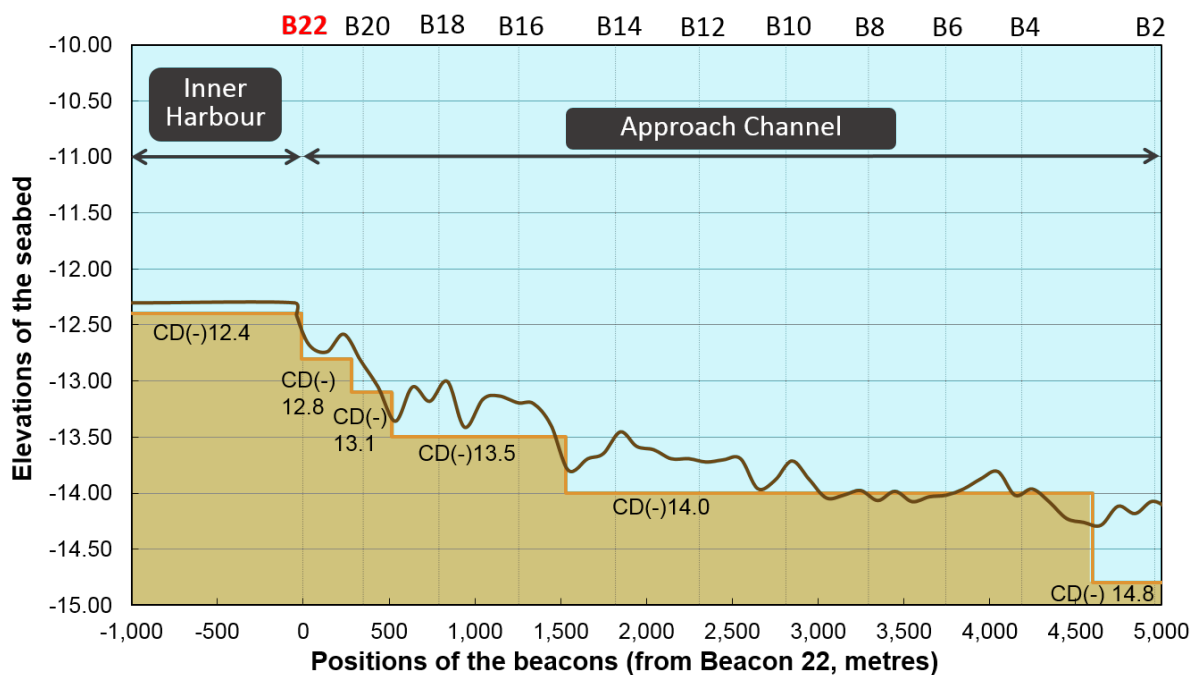


Figure 4. A comparison of the seabed lines based on the chart and the survey.

4. DATA PROCESSING

All data recorded at 1.0 Hz was post-processed. The raw GNSS results for each receiver have been combined to give the sinkage at the Forward Perpendicular (FP), Aft Perpendicular (AP), and forward and aft shoulder of the bilge corners that would be a point of concern of running aground. No additional hogging or sagging of the ship while underway is considered. A method and important height components for calculating sinkage from the raw GNSS height measurements are described in Appendix F.

Note that gaps in the data of some transits are due to GNSS fixes being of insufficient quality and being rejected.

5. RESULTS

5.1. Measured ship tracks

Layout of the Port of Geraldton, its approach channel and navigational beacons, together with tracks of the five inbound ships and the six outbound ships are illustrated in Appendix C. The channel is around 2.8 nautical miles in length and 180m in width (at toe of bottom slope), varying in depth from 12.4m to 14.8m based on the Chart Datum, which is approximately the level of LAT (Lowest Astronomical Tide). An additional depth of up to 1.2m can be considered by tides, i.e. HAT (Highest Astronomical Tide) and MSL (Mean Sea Level) in the Port of Geraldton are 1.2m and 0.6m respectively (see chart AUS81).

The measurements for the inbound ships were made from the moment all onboard receivers are set up, which is invariably before the ships move into the channel (or pass Beacon 1 and 2), until all mooring work is completed at the berth. For the outbound ships, the measurements were made from the berth until the ships pass the last beacons (Beacon 1 and 2) at the end of the channel.

5.2. Individual measurement results

Measured sinkage, together with ship speed and channel bathymetry, are shown in Appendix D. Sinkage is given at the FP, AP, and forward and aft shoulder of the bilge corners and defined as being positive downward. Here, dynamic sinkage means the total sinkage, relative to the static floating position at the berth, that includes: a near-steady component due to the Bernoulli effect known as squat; an unsteady component due to wave-induced heave, pitch and roll; and a slowly-varying heel due to wind and turning. Results are plotted against cumulative distance from Beacon 22, located at the entrance of the channel (see Figure 3). Distance within the harbour, therefore, is negative. Vertical lines are shown for Beacon 20, Beacon 18, Beacon 16, ..., Beacon 2.

For practical UKC management, the ship's vertical position should be plotted, relative to Chart Datum, so that the port may know the actual real-time clearance from the seabed. Appendix D also includes these vertical elevation changes. The minimum real-time clearance in each section of varying water depth has been captured.

Maximum sinkage results for the ship transits are shown in Table 1.

Table 1. Measured maximum sinkage and dynamic draught, and dynamic draught increase for the ship transits.

Ships	In/ Out	Maximum sinkage			Maximum dynamic draught		Dynamic draught increase	
		metres	point	% of static draught	metres	point	metres	% of static draught
HONG YUAN	in	0.65	AP	7.16	9.77	AP	0.65	7.16
PETANI		0.65	AP	7.94	8.85	AP	0.65	7.94
DONNACONA		0.43	Stbd Fwd Bilge	4.72	9.70	AP	0.41	4.37
AAL FREMANTLE		0.90	AP	14.88	6.97	AP	0.90	14.88
SEA DIAMOND		0.80	AP	10.42	8.45	AP	0.80	10.42
GUO DIAN 17	out	0.77	FP	6.31	12.92	FP	0.77	6.31
SFL SPEY		1.05	FP	12.79	9.27	FP	1.05	12.79
IVS MAGPIE		0.98	Port Fwd Bilge	11.16	9.77	Port Fwd Bilge	0.98	11.16
FENG HUANG FENG		0.56	FP	4.57	12.74	FP	0.56	4.57
AAL FREMANTLE		0.58	FP	6.66	9.89	AP	0.41	4.30
SEA DIAMOND		0.94	FP	10.60	11.10	AP	0.84	8.22

Nearly half of the transits have maximum sinkage at the stern, and the other half at the bow, according to directions of inbound or outbound. However, for a ship with static stern-down trim, e.g. DONNACONA inbound, AAL FREMANTLE outbound and SEA DIAMOND outbound (see Appendix A), the FP or forward shoulder of the bilge corners having maximum sinkage may not be the closest point to the seabed. The stern can still have maximum dynamic draught due to its already close proximity to the seabed. Here, the dynamic draught at each location on the ship can be found by adding the static draught at that point to the sinkage at that point. The point on the ship with the maximum dynamic draught is the point most likely to hit the bottom, shown in Table 1.

Dynamic draught increase is, here, defined as the difference between the maximum dynamic draught and its static draught. This leads directly to decrease in UKC, and hence is the most important consideration in avoiding grounding. Maximum sinkage and dynamic draught increase are also expressed as a percentage of the static draught of the ships to compare the results to conventional information on ship UKC or navigation.

Calculated minimum real-time clearance in the inner harbour and approach channel, as well as the keel point where that occurs, are shown in Table 2.

Table 2. Calculated minimum UKC for the ship transits.

Ships	In/ Out	Inner harbour			Approach channel		
		metres	point	% of static draught	metres	point	% of static draught
HONG YUAN	in	3.49	AP	38.23	3.92	AP	42.93
PETANI		4.49	AP	54.74	4.85	AP	59.13
DONNACONA		3.43	AP	36.95	3.83	AP	41.17
AAL FREMANTLE		6.72	Port Aft Bilge	111.02	7.07	AP	116.41
SEA DIAMOND		4.99	AP	65.17	5.22	AP	68.26
GUO DIAN 17	out	0.80	Stbd Fwd Bilge	6.61	1.01	FP	8.35
SFL SPEY		4.70	AP	56.87	4.93	FP	59.97
IVS MAGPIE		3.92	AP	44.43	4.34	Stbd Fwd Bilge	49.34
FENG HUANG FENG		0.90	Stbd Aft Bilge	7.40	1.30	AP	10.64
AAL FREMANTLE		3.53	AP	37.19	3.89	AP	40.99
SEA DIAMOND		2.25	AP	21.94	2.62	AP	25.57

Generally, for the ships trimmed by the stern at departure or arrival time, the AP is the closest point to the seabed in both harbour and channel, but the ships with almost level static trim, e.g. GUO DIAN 17 outbound, SFL SPEY outbound and IVS MAGPIE outbound, have their minimum UKC at the FP or the forward shoulder of the bilge corners in the channel.

5.3. Comparisons between the transits

With dynamic sinkage at six points of the ships, we have also calculated dynamic trim and heel of all the transits. Appendix E has been made for comparing these results between each of the transits and falls into the categories of inbound and outbound transits.

Dynamic trim means, here, the ship's total change in trim (positive stern-down), relative to the static floating position at the berth, that includes wave-induced pitch. Note that dynamic trim is given in metres based on the difference between the FP and AP. Dynamic heel is the ship's total change in heel (positive to starboard), relative to the static floating position at the berth, that includes wave-induced roll, and given in degrees.




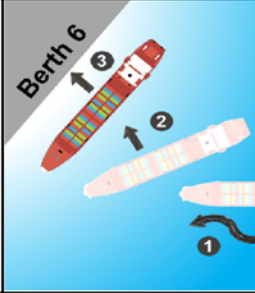

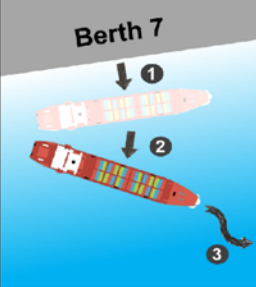
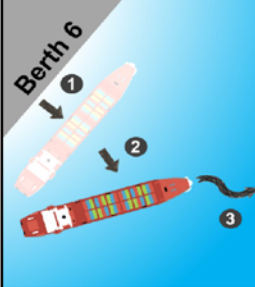
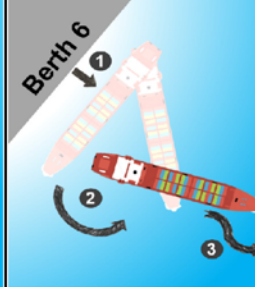
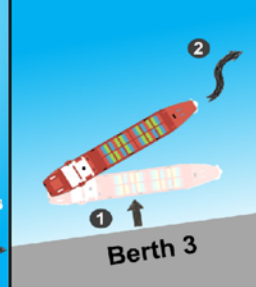
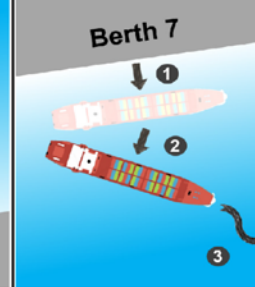
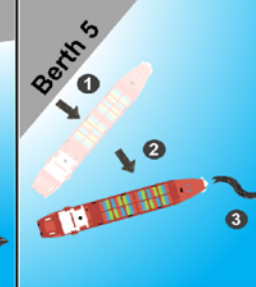
Additionally, for a better understanding of dynamic heel, natural roll period of the ship transits should be calculated and compared with the wave period measured during each trial, as shown in Table 3. Resonant rolling can occur for a ship when the wave encounter period is close to the ship's natural roll period. The natural roll period T_ϕ is described in more detail in Appendix F. The wave data in Table 3 and Appendix B is from the same source.

Table 3. Calculated natural roll period and measured wave data during each measurement.

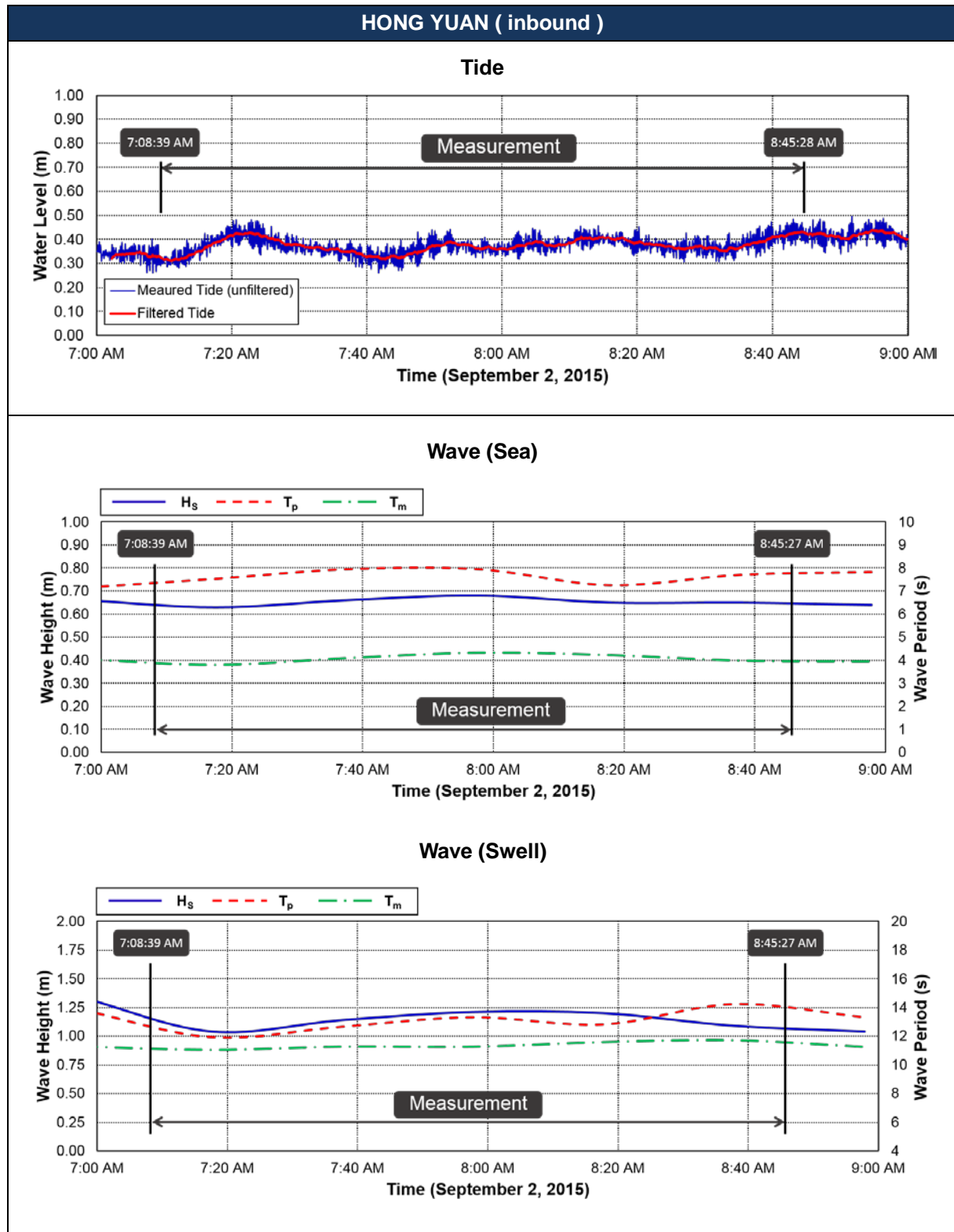
Ships	In/ Out	GM _f (m)	Natural roll period (T_ϕ , sec)	Measured wave data (Swell)	
				T_p (sec)	T_m (sec)
HONG YUAN	in	4.13	12.70	11.9 ~ 14.2	11.0 ~ 11.7
PETANI		3.86	13.14	10.7 ~ 12.3	10.7 ~ 11.4
DONNACONA		2.55	12.27	10.1 ~ 13.0	11.1 ~ 12.2
AAL FREMANTLE		2.44	11.98	9.7 ~ 13.8	11.3 ~ 12.0
SEA DIAMOND		5.04	11.50	11.1 ~ 13.1	11.6 ~ 12.2
GUO DIAN 17	out	7.11	9.68	9.2 ~ 14.2	11.0 ~ 11.9
SFL SPEY		6.71	9.27	11.9 ~ 14.2	11.4 ~ 11.8
IVS MAGPIE		3.08	12.40	11.5 ~ 14.0	11.2 ~ 11.8
FENG HUANG FENG		7.10	9.69	10.8 ~ 13.5	11.0 ~ 11.5
AAL FREMANTLE		2.29	12.37	10.0 ~ 18.6	11.0 ~ 11.5
SEA DIAMOND		5.93	10.60	13.1 ~ 15.1	13.0 ~ 14.0

T_p is the peak energy wave period, and T_m is the mean wave period. GM_f is metacentric height, corrected for free surface effect.

Appendix A – Details of the ships and transit conditions

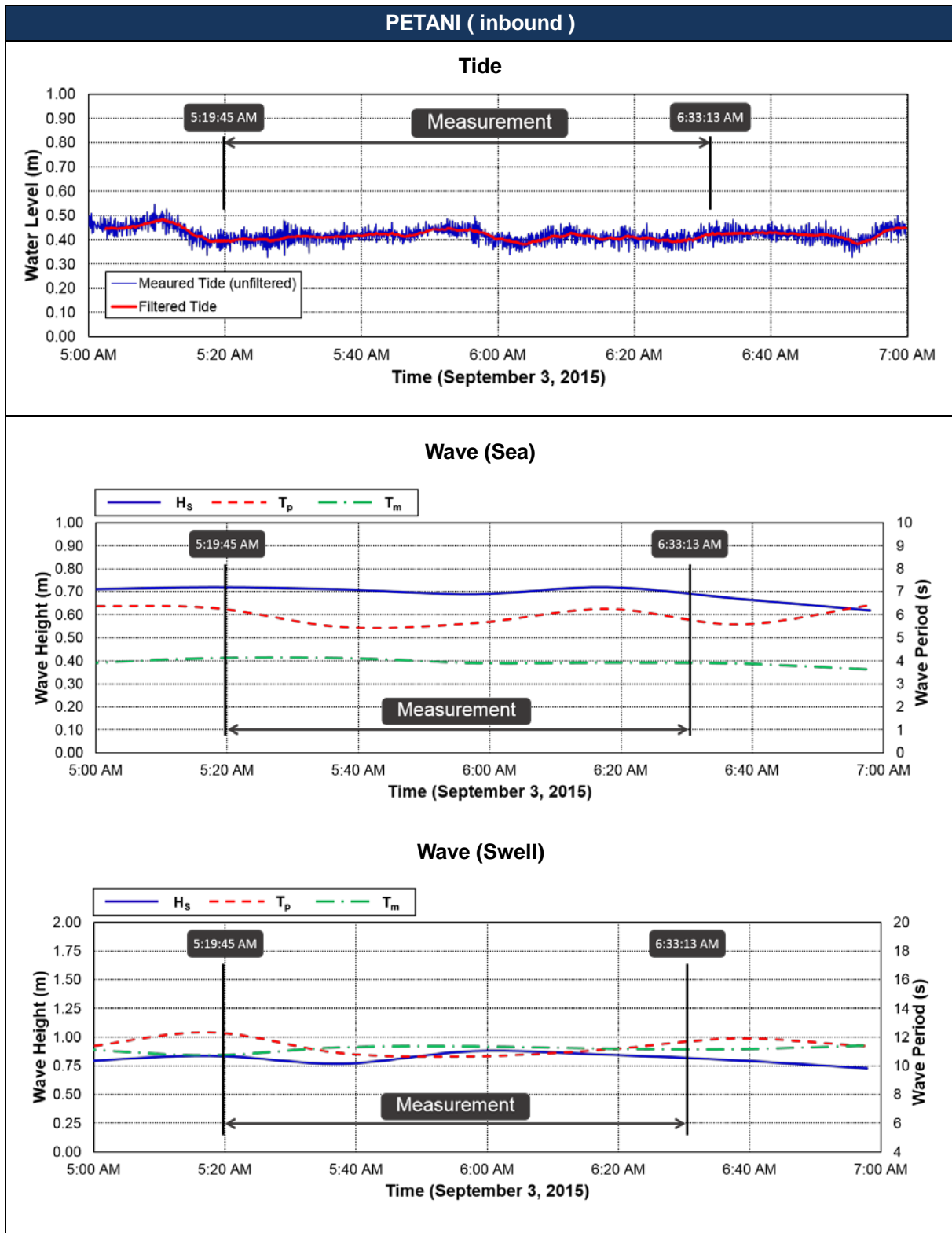
	HONG YUAN		PETANI		DONNACONA		GUO DIAN 17		SFL SPEY		AAL FREMANTLE		IVS MAGPIE		FENG HUANG FENG		SEA DIAMOND	
Ship Type	Panamax		Panamax		Handy		Panamax		Handy		Handy		Handy		Panamax		Panamax	
Capacity (DWT)	76,364		75,228		28,115		76,426		33,986		18,793		28,240		75,396		77,096	
Year Built	2009		2008		2001		2013		2011		2011		2011		2011		2007	
L _{OA} (m)	225.00		225.00		166.30		225.00		181.00		148.60		169.37		225.00		224.99	
L _{PP} (m)	217.00		217.00		161.15		219.00		172.00		140.30		160.40		217.00		217.00	
Depth (m)	19.60		-		-		19.60		14.00		13.50		13.60		19.60		19.50	
Beam (m)	32.26		32.26		24.50		32.26		30.00		23.40		27.20		32.26		32.26	
Design Draught (m)	12.20		12.50		-		12.20		9.40		8.00		-		12.20		12.24	
Summer Draught (m)	14.20		14.20		10.51		14.20		9.82		9.80		9.82		14.22		14.08	
Displacement (ton) at summer draught	88,500.00		87,003.00		35,407.00		89,800.80		-		26,553.30		34,766.00		88,535.90		87,782.00	
Arrival Draught (m)	FP	7.34	FP	7.30	FP	9.18	-	-	FP	6.02	-	-	-	-	-	-	FP	5.65
	Mid	8.25	Mid	7.75	Mid	9.24			Mid	6.05							Mid	6.65
	AP	9.12	AP	8.20	AP	9.29			AP	6.07							AP	7.65
Departure Draught (m)	-		-		-		FP	12.15	FP	8.22	FP	8.75	FP	8.78	FP	12.18	FP	8.91
							Mid	12.15	Mid	8.25	Mid	9.11	Mid	8.80	Mid	12.20	Mid	-
							AP	12.15	AP	8.27	AP	9.48	AP	8.82	AP	12.20	AP	10.26
Berth No.	No.7		No.5		No.6		No.7		No.6		No.6		No.3		No.7		No.5	
Berthing side (port or stbd)	port-side		port-side		port-side		port-side		port-side		starboard-side		starboard-side		port-side		port-side	
Arrival Berthing							-		-				-		-			
Departure Unberthing	-		-		-													

Appendix B – Tidal and wave (sea/swell) data



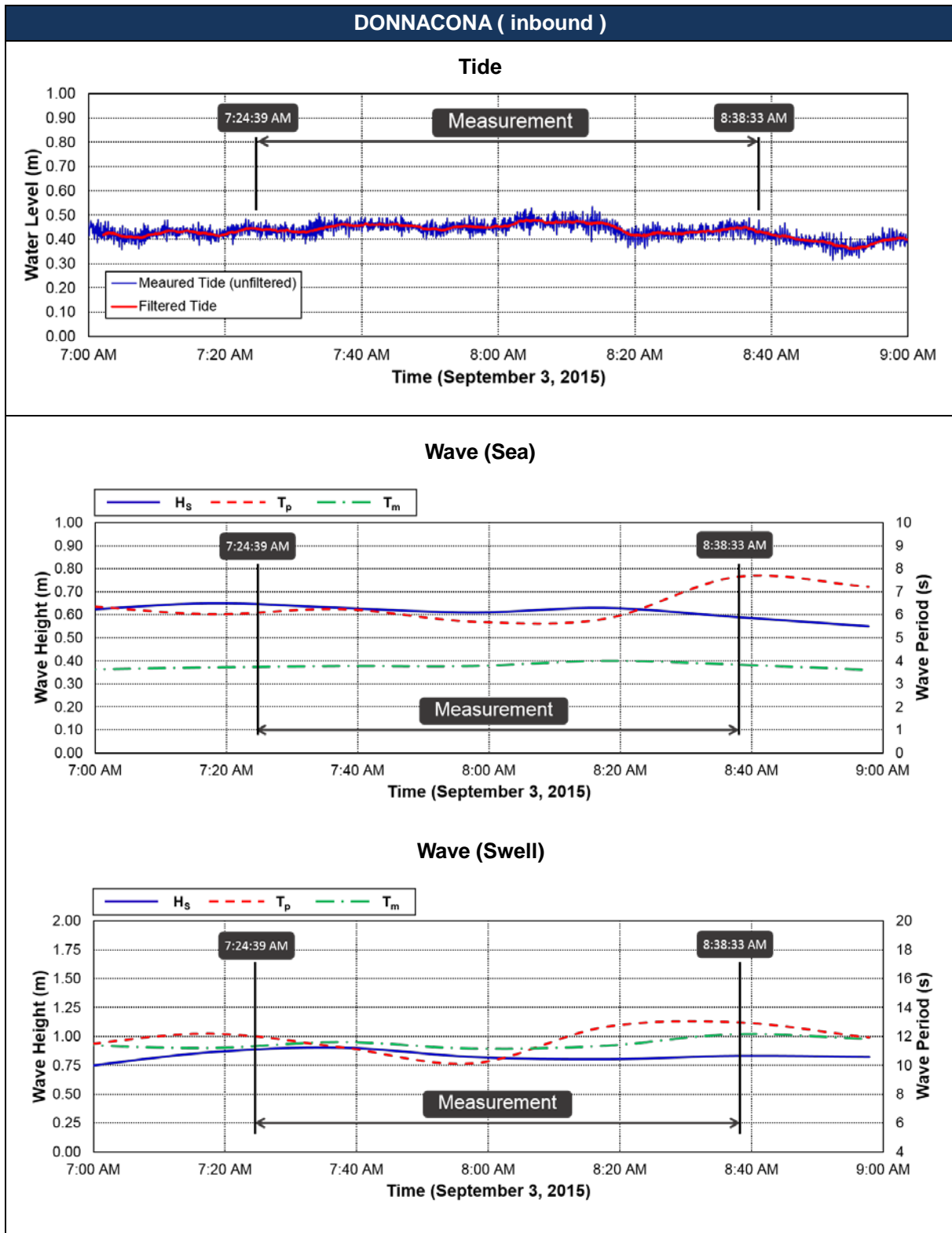
<Top> Raw sea surface elevations as measured at Berth 3-4, and filtered tide using a low-pass filter with a cutoff period of 5 minutes.

<Bottom> Measured wave data from the AWAC at Beacon 2. Sea/swell cutoff is 8 seconds. H_s is the significant wave height, T_p is the peak energy wave period, and T_m is the mean wave period.



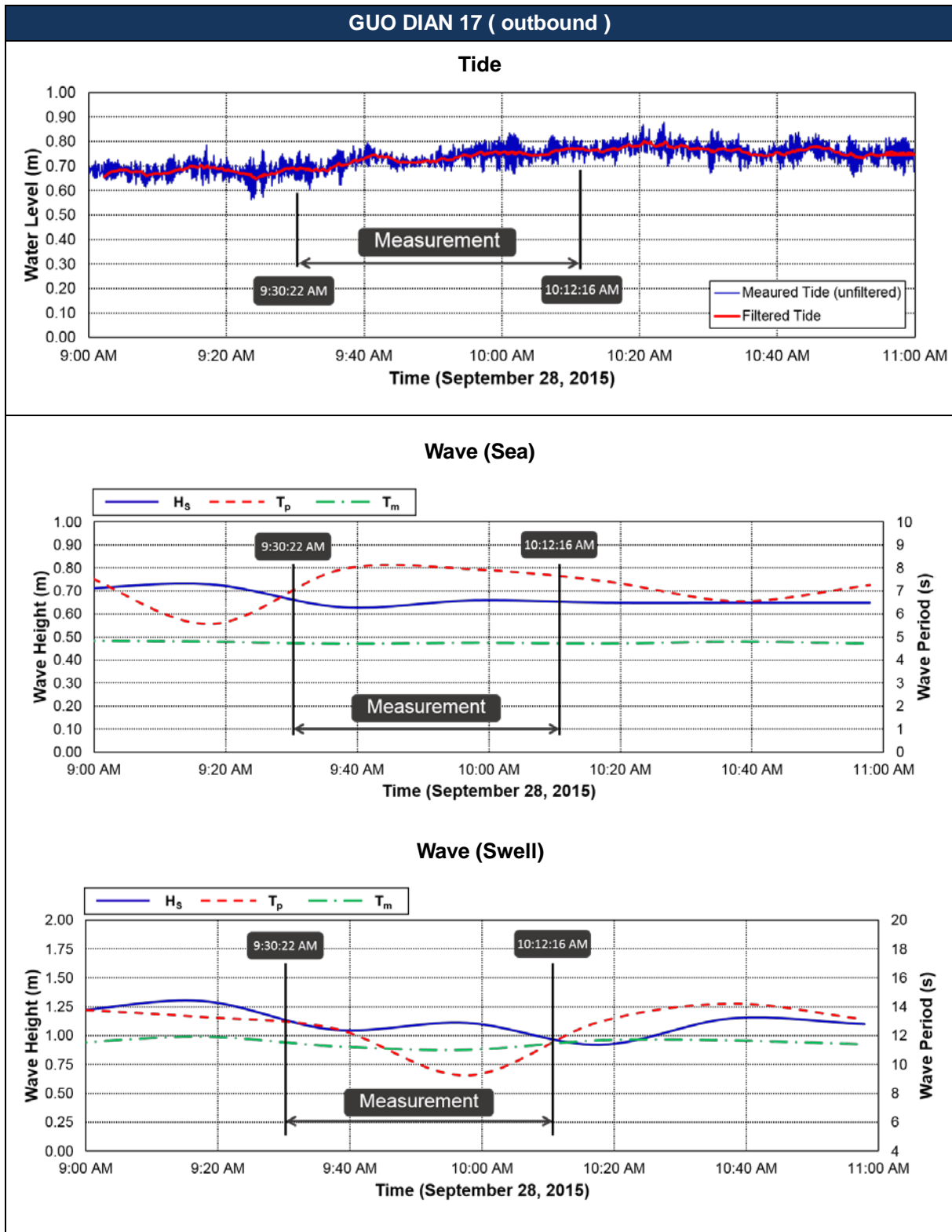
<Top> Raw sea surface elevations as measured at Berth 3-4, and filtered tide using a low-pass filter with a cutoff period of 5 minutes.

<Bottom> Measured wave data from the AWAC at Beacon 2. Sea/swell cutoff is 8 seconds. H_s is the significant wave height, T_p is the peak energy wave period, and T_m is the mean wave period.



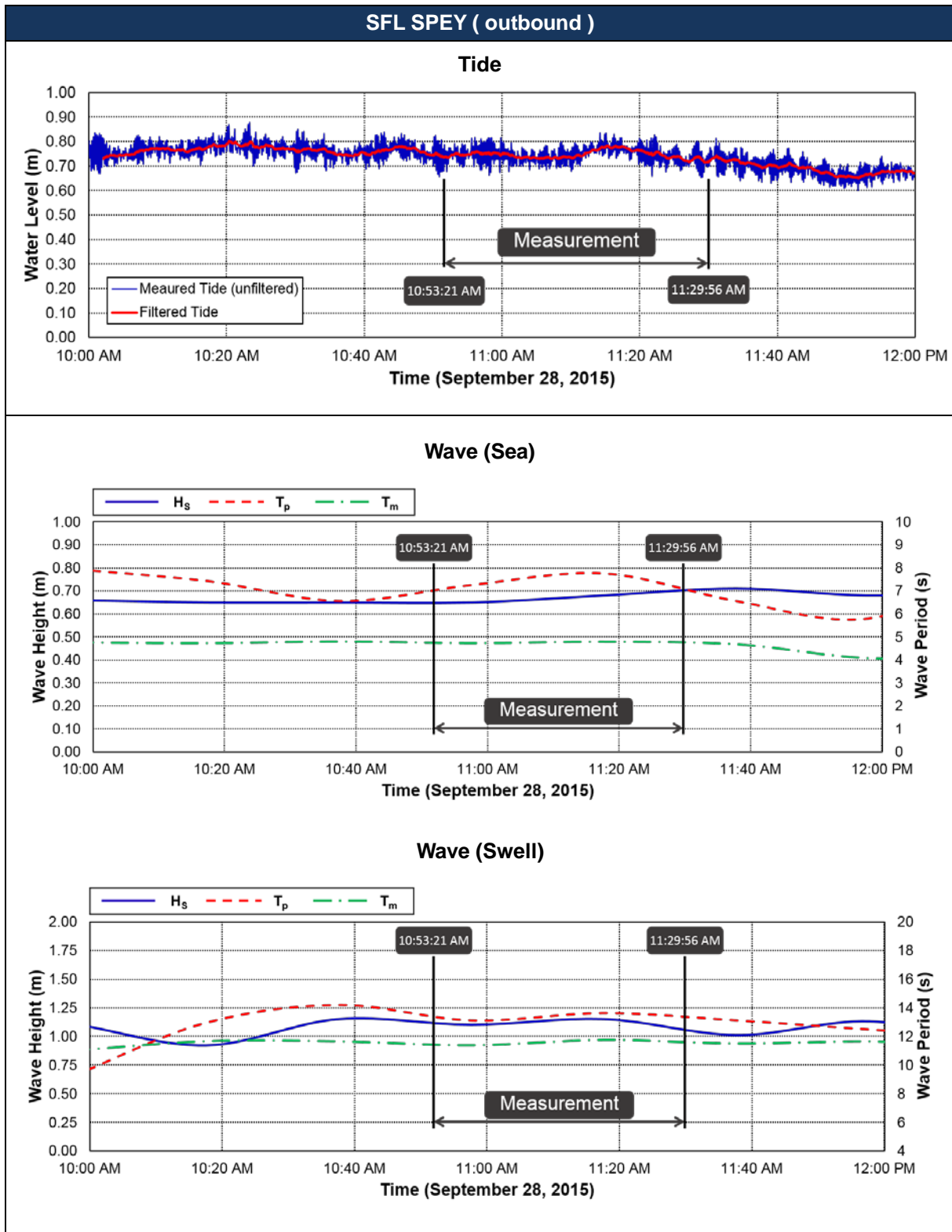
<Top> Raw sea surface elevations as measured at Berth 3-4, and filtered tide using a low-pass filter with a cutoff period of 5 minutes.

<Bottom> Measured wave data from the AWAC at Beacon 2. Sea/swell cutoff is 8 seconds. H_s is the significant wave height, T_p is the peak energy wave period, and T_m is the mean wave period.



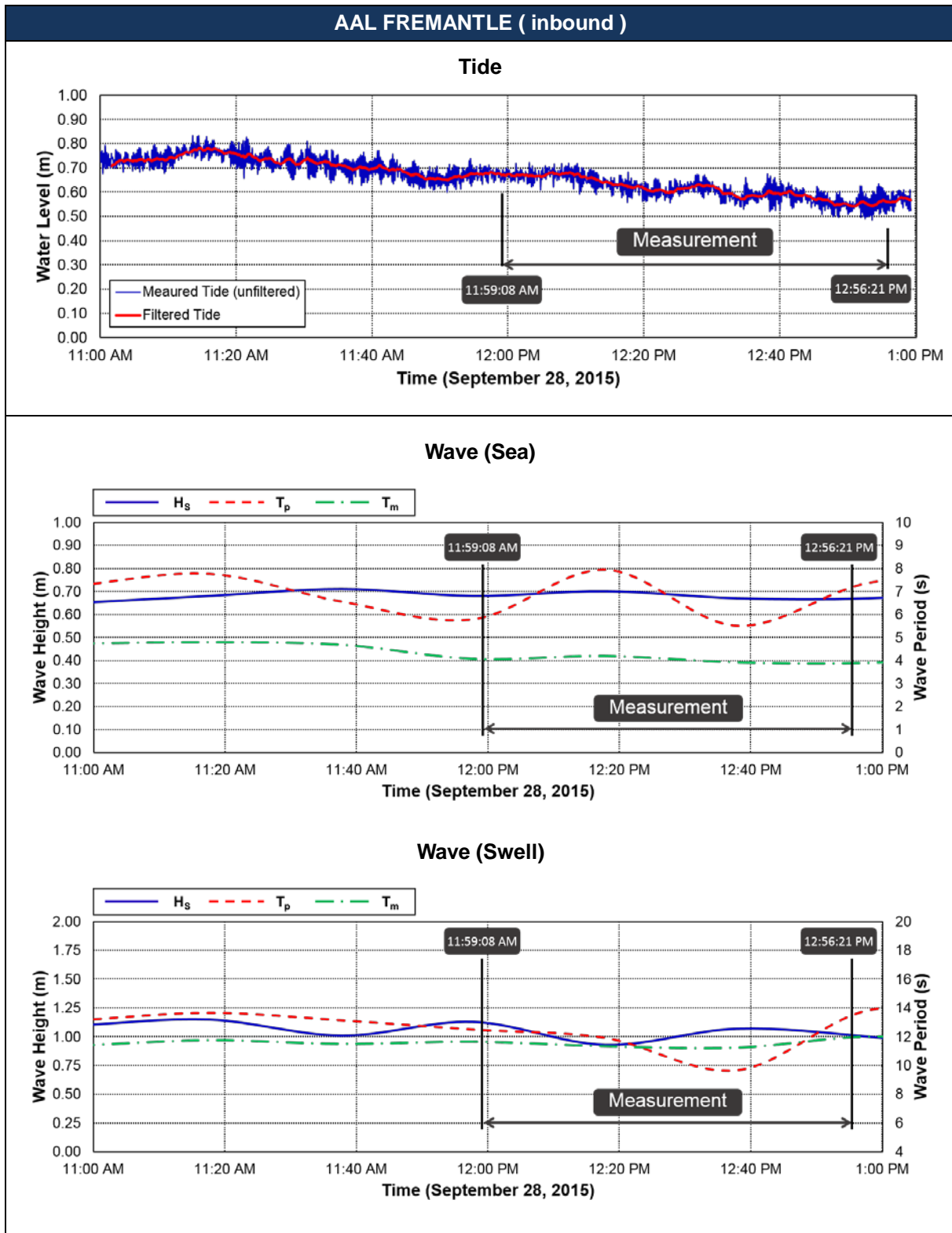
<Top> Raw sea surface elevations as measured at Berth 3-4, and filtered tide using a low-pass filter with a cutoff period of 5 minutes.

<Bottom> Measured wave data from the AWAC at Beacon 2. Sea/swell cutoff is 8 seconds. H_s is the significant wave height, T_p is the peak energy wave period, and T_m is the mean wave period.



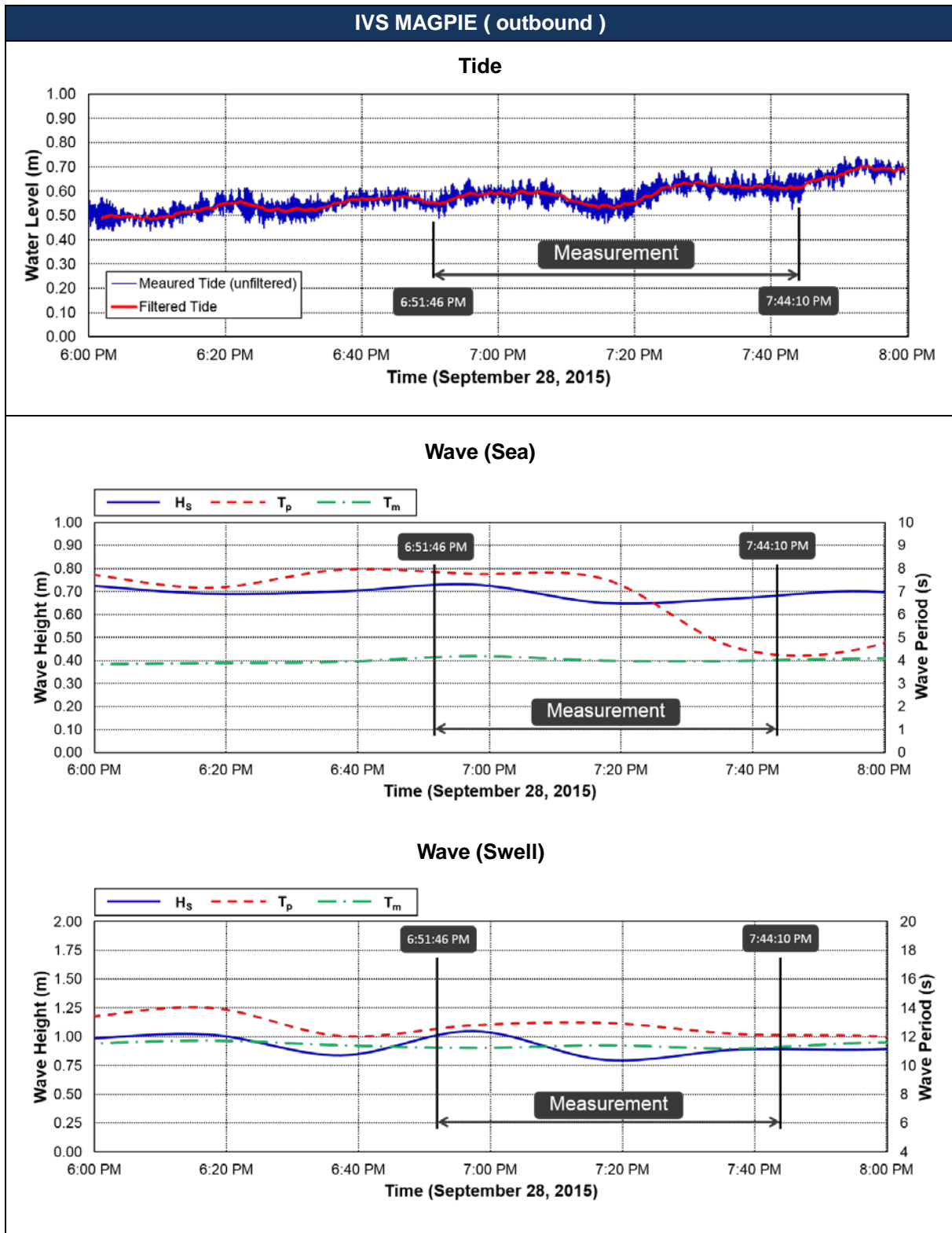
<Top> Raw sea surface elevations as measured at Berth 3-4, and filtered tide using a low-pass filter with a cutoff period of 5 minutes.

<Bottom> Measured wave data from the AWAC at Beacon 2. Sea/swell cutoff is 8 seconds. H_s is the significant wave height, T_p is the peak energy wave period, and T_m is the mean wave period.



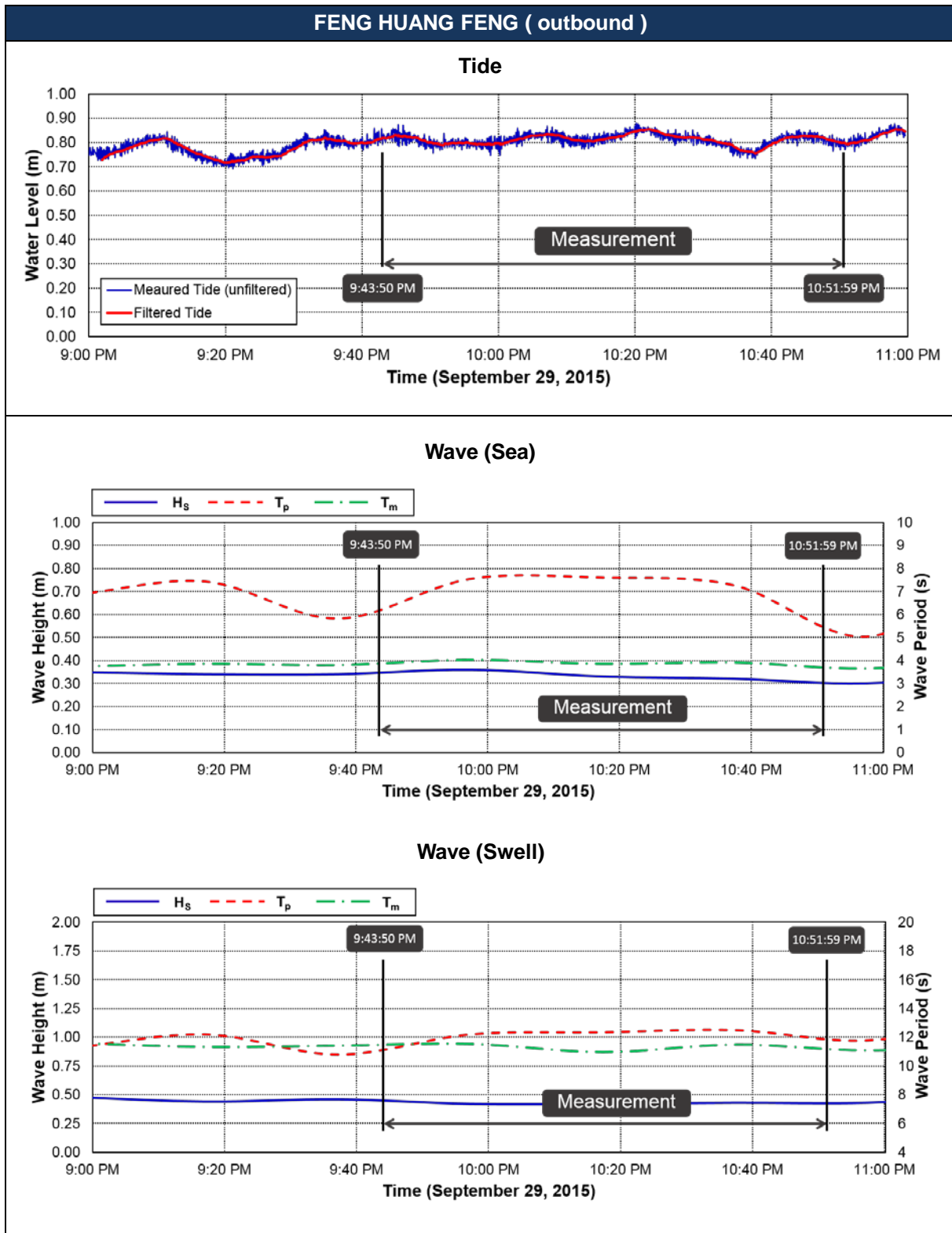
<Top> Raw sea surface elevations as measured at Berth 3-4, and filtered tide using a low-pass filter with a cutoff period of 5 minutes.

<Bottom> Measured wave data from the AWAC at Beacon 2. Sea/swell cutoff is 8 seconds. H_s is the significant wave height, T_p is the peak energy wave period, and T_m is the mean wave period.



<Top> Raw sea surface elevations as measured at Berth 3-4, and filtered tide using a low-pass filter with a cutoff period of 5 minutes.

<Bottom> Measured wave data from the AWAC at Beacon 2. Sea/swell cutoff is 8 seconds. H_s is the significant wave height, T_p is the peak energy wave period, and T_m is the mean wave period.

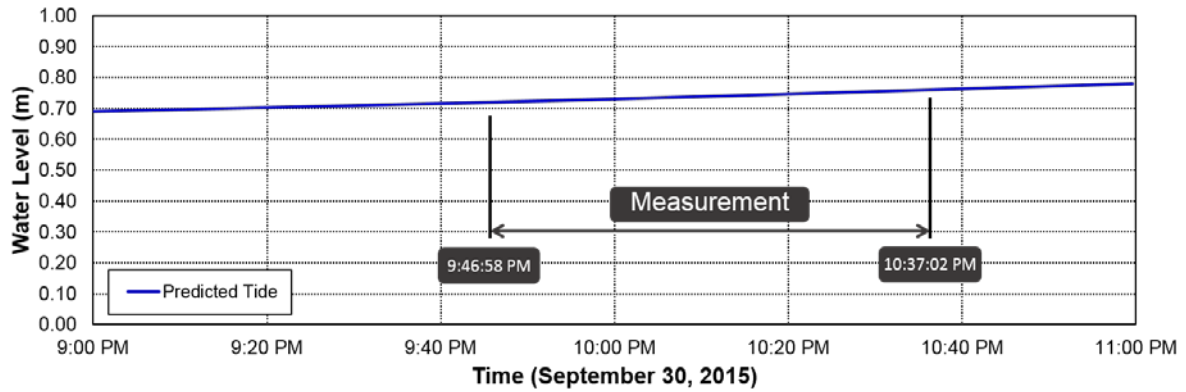


<Top> Raw sea surface elevations as measured at Berth 3-4, and filtered tide using a low-pass filter with a cutoff period of 5 minutes.

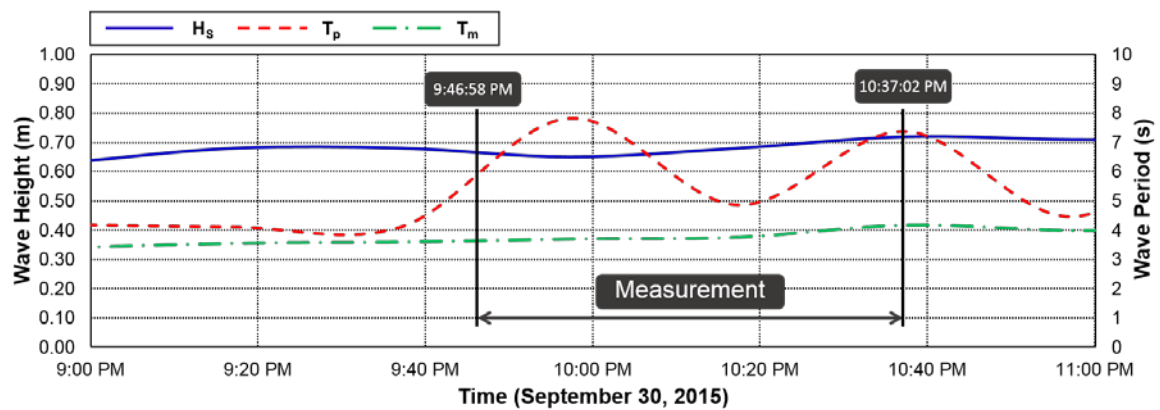
<Bottom> Measured wave data from the AWAC at Beacon 2. Sea/swell cutoff is 8 seconds. H_s is the significant wave height, T_p is the peak energy wave period, and T_m is the mean wave period.

AAL FREMANTLE (outbound)

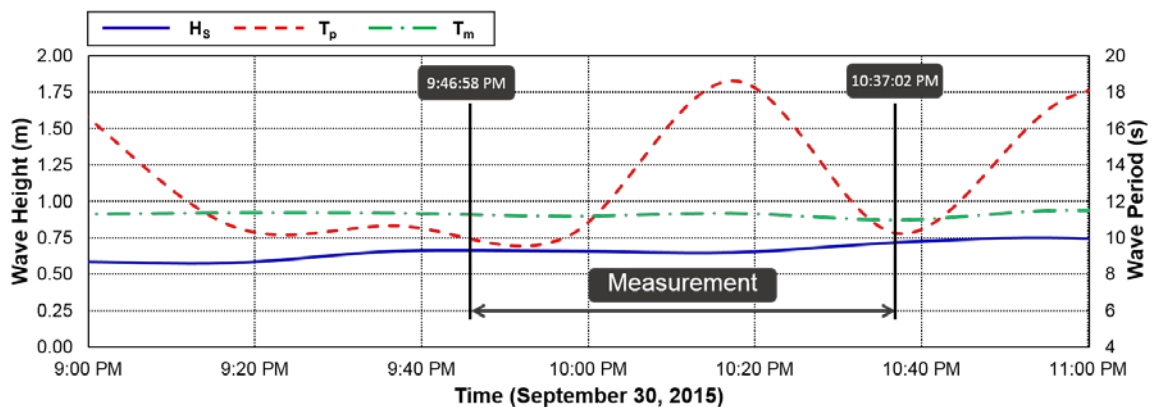
Tide



Wave (Sea)

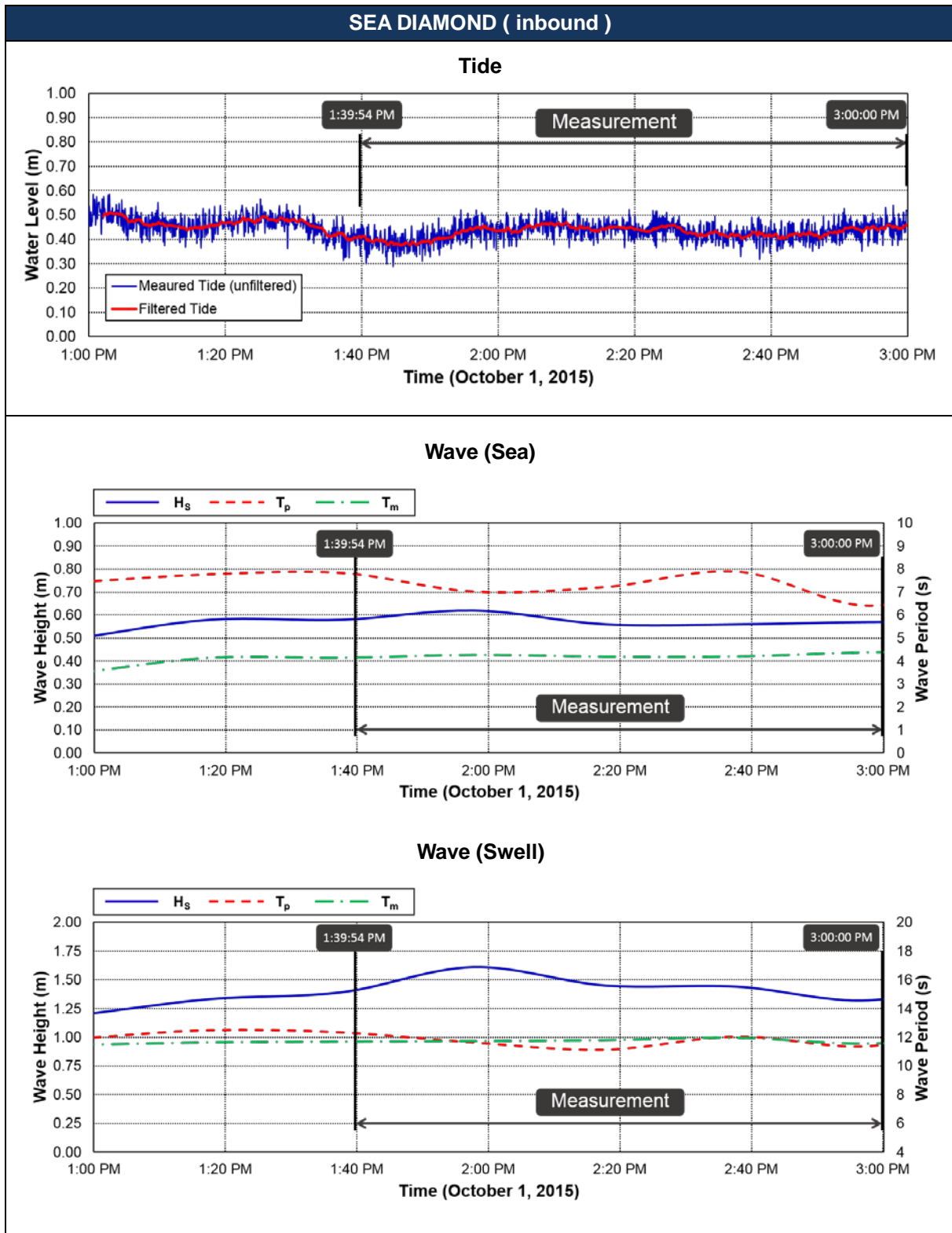


Wave (Swell)



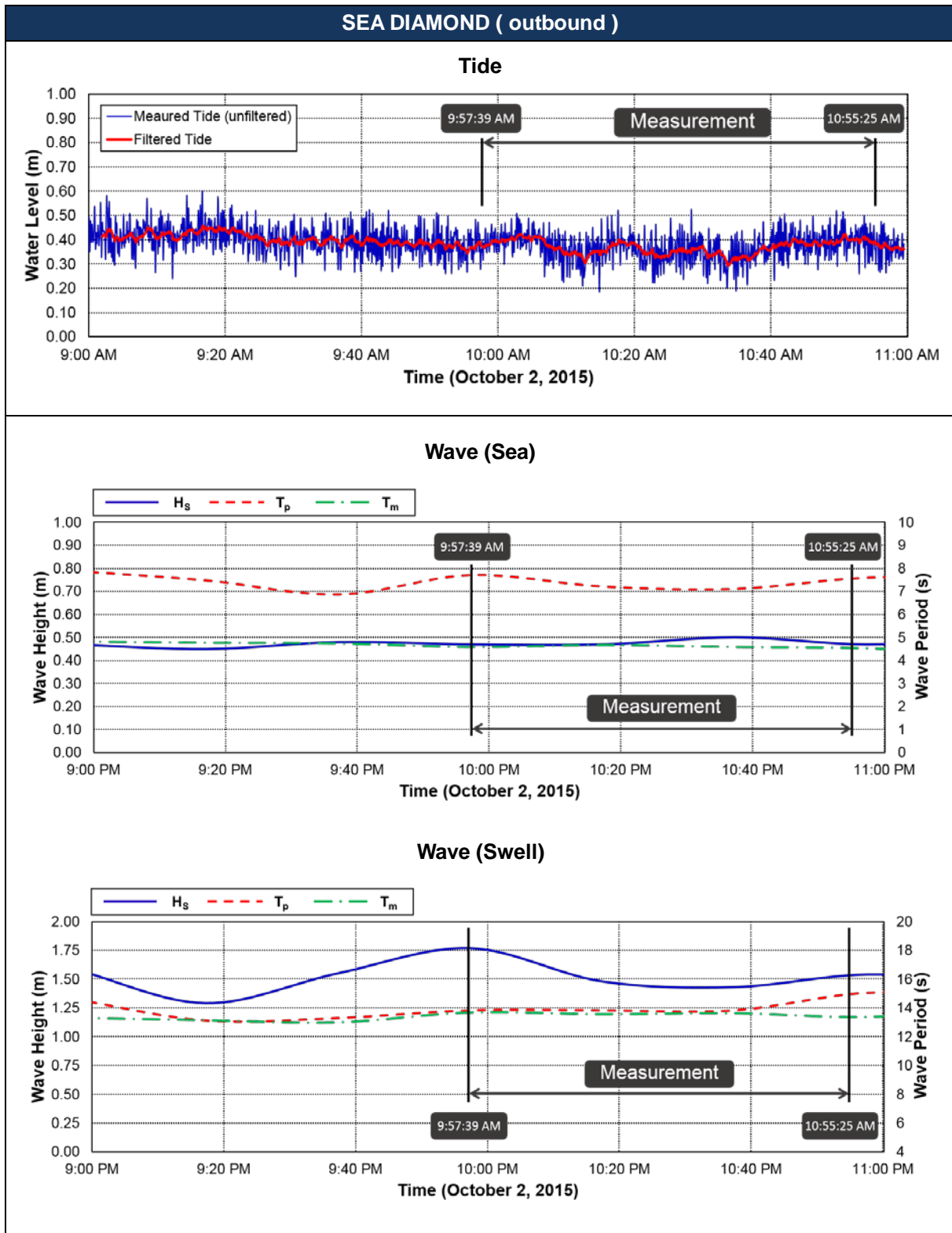
<Top> Hourly tidal elevation predictions for Geraldton from the Australian Government Bureau of Meteorology (BoM).

<Bottom> Measured wave data from the AWAC at Beacon 2. Sea/swell cutoff is 8 seconds. H_s is the significant wave height, T_p is the peak energy wave period, and T_m is the mean wave period.



<Top> Raw sea surface elevations as measured at Berth 3-4, and filtered tide using a low-pass filter with a cutoff period of 5 minutes.

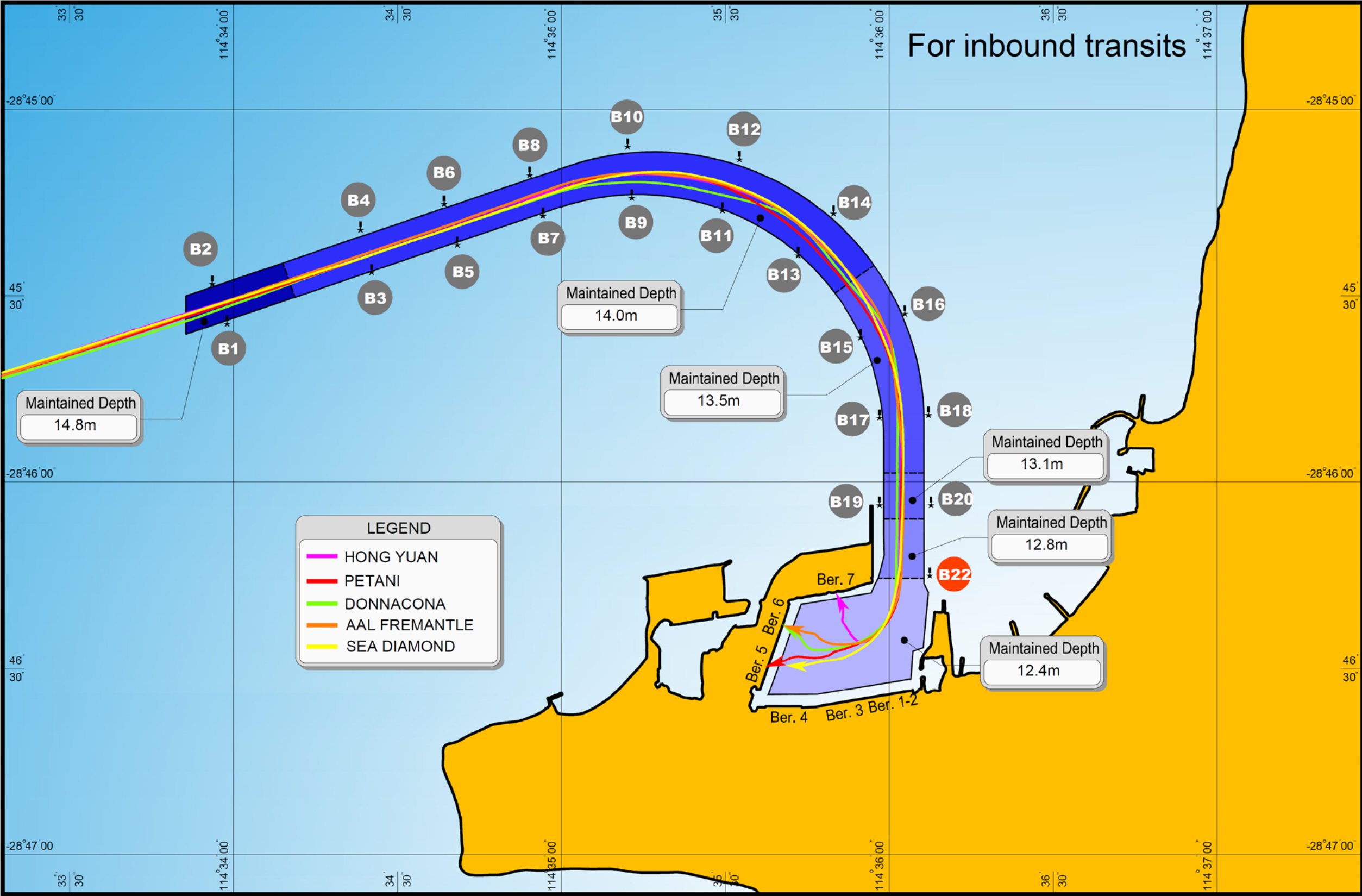
<Bottom> Measured wave data from the AWAC at Beacon 2. Sea/swell cutoff is 8 seconds. H_s is the significant wave height, T_p is the peak energy wave period, and T_m is the mean wave period.

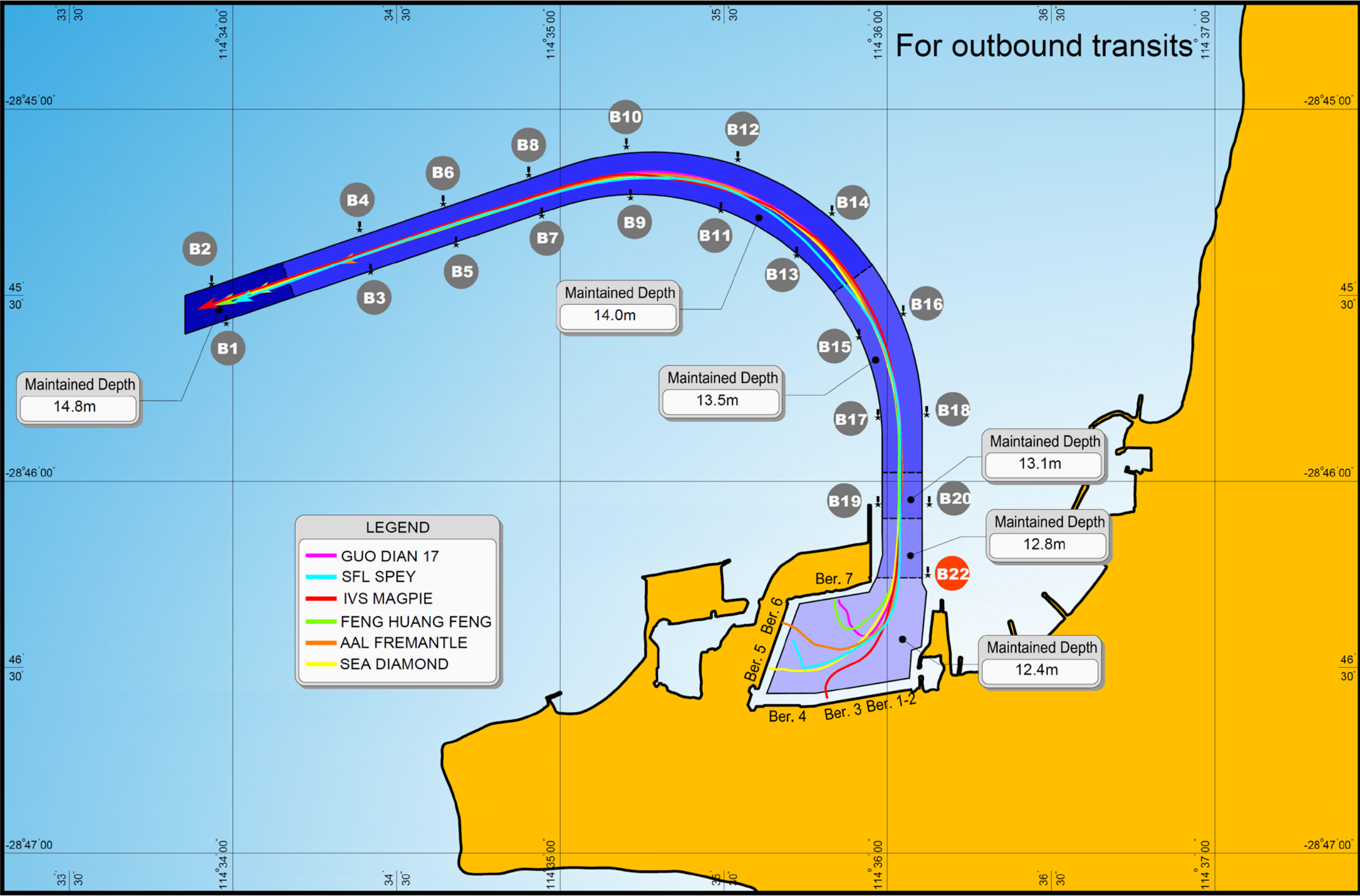


<Top> Raw sea surface elevations as measured at Berth 3-4, and filtered tide using a low-pass filter with a cutoff period of 5 minutes.

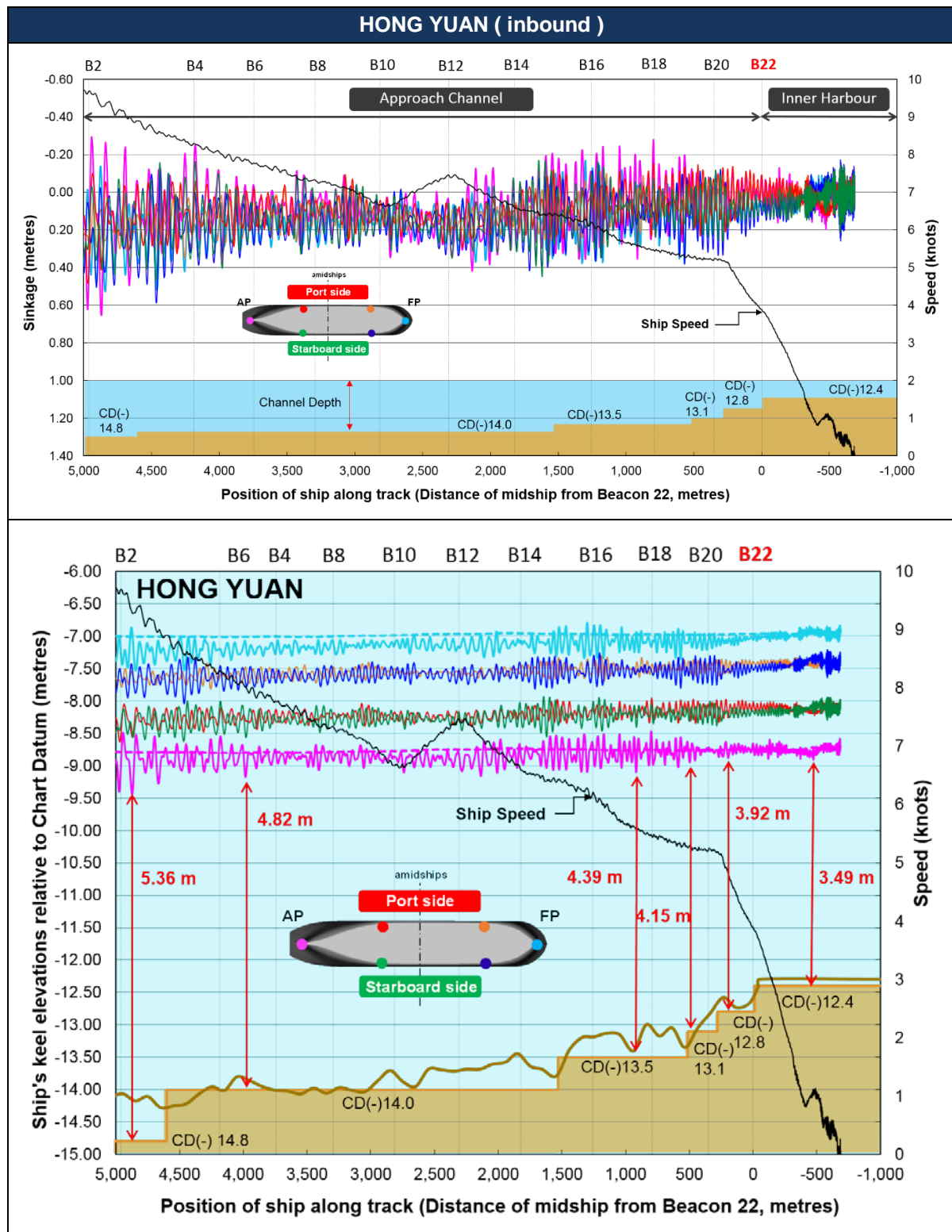
<Bottom> Measured wave data from the AWAC at Beacon 2. Sea/swell cutoff is 8 seconds. H_s is the significant wave height, T_p is the peak energy wave period, and T_m is the mean wave period.

Appendix C – Measured ship tracks



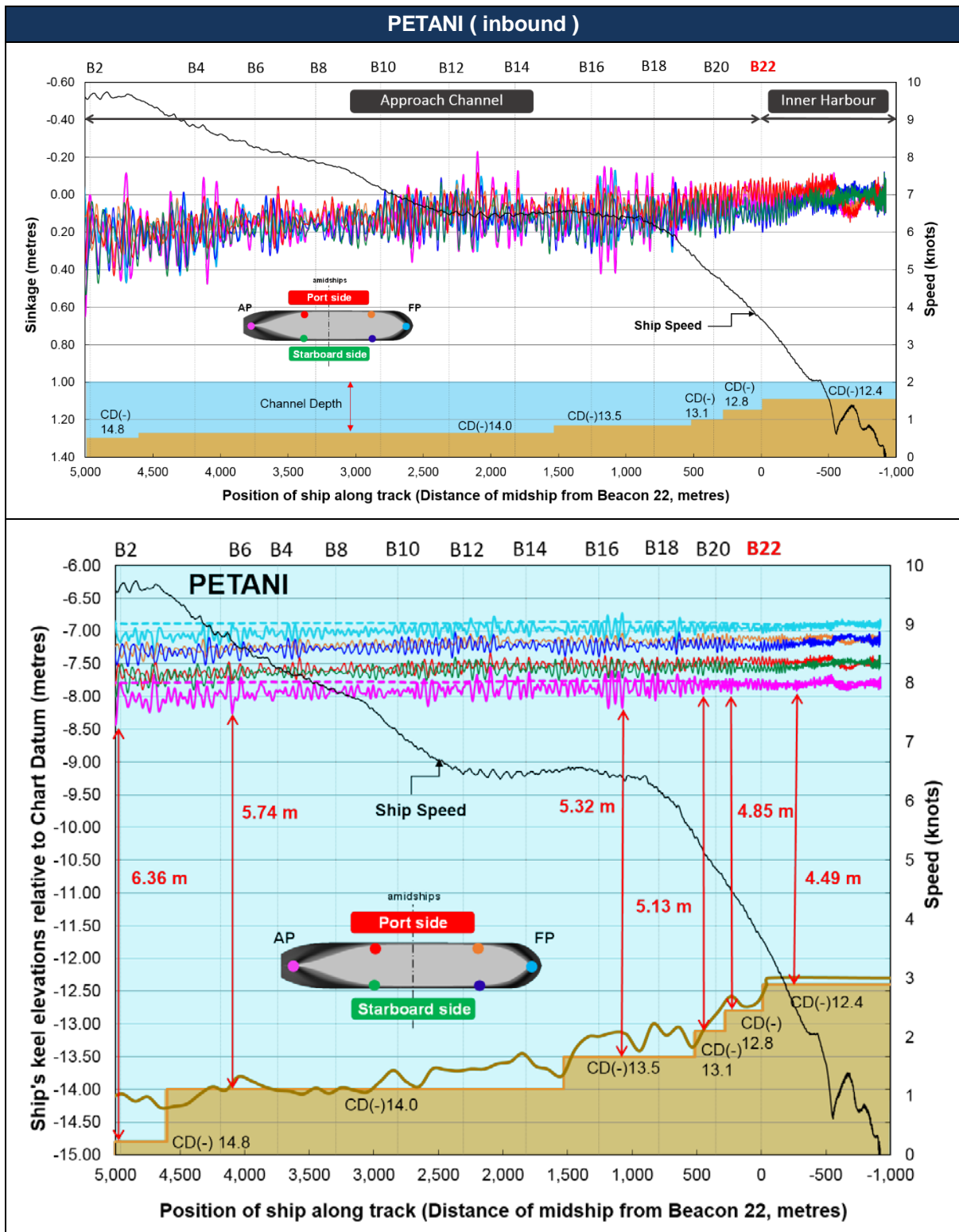


Appendix D – Measured dynamic sinkage and UKC (Graphical results)



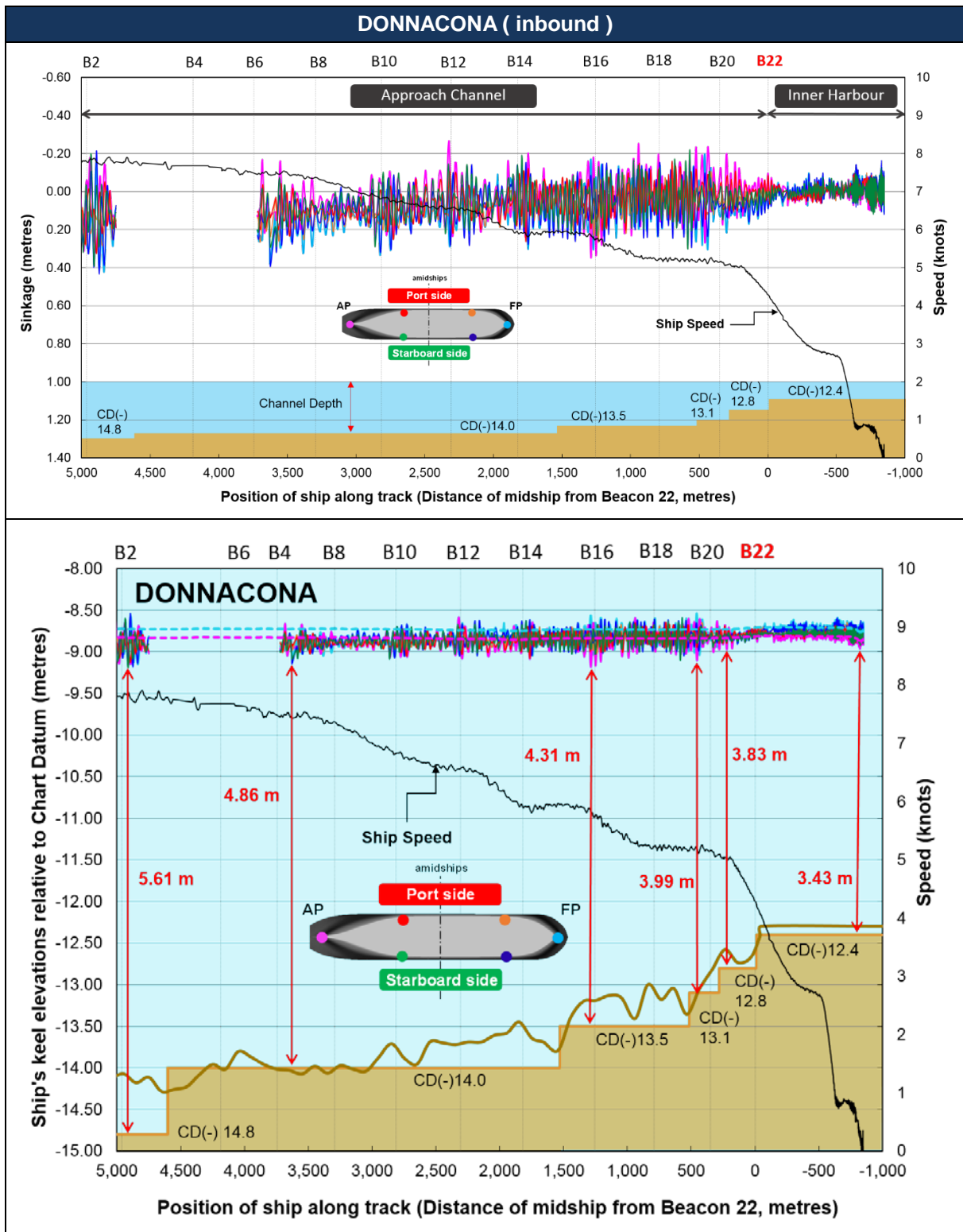
<Top> Measured sinkage (positive downward) at six points. Chart datum depths (not to scale) also shown.

<Bottom> Elevation of the ship's keel relative to chart datum. Broken lines are elevations of the FP and AP including changes in tide only, i.e. their static position, not including squat and wave-induced motions. A flat seabed line is based on the charted depth on AUS 81, and a fluctuating seabed line is the actual survey line provided by OMC International.



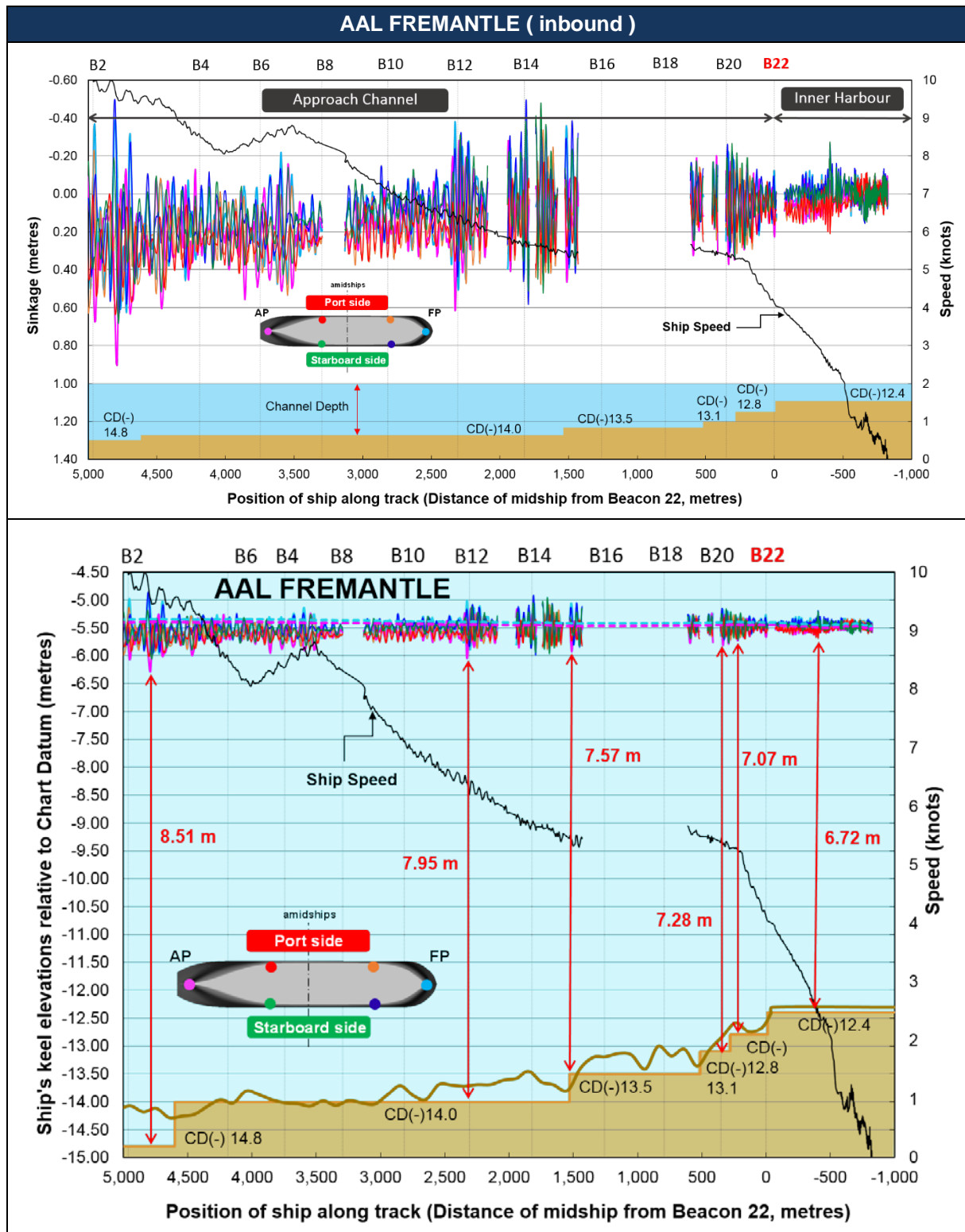
<Top> Measured sinkage (positive downward) at six points. Chart datum depths (not to scale) also shown.

<Bottom> Elevation of the ship's keel relative to chart datum. Broken lines are elevations of the FP and AP including changes in tide only, i.e. their static position, not including squat and wave-induced motions. A flat seabed line is based on the charted depth on AUS 81, and a fluctuating seabed line is the actual survey line provided by OMC International.



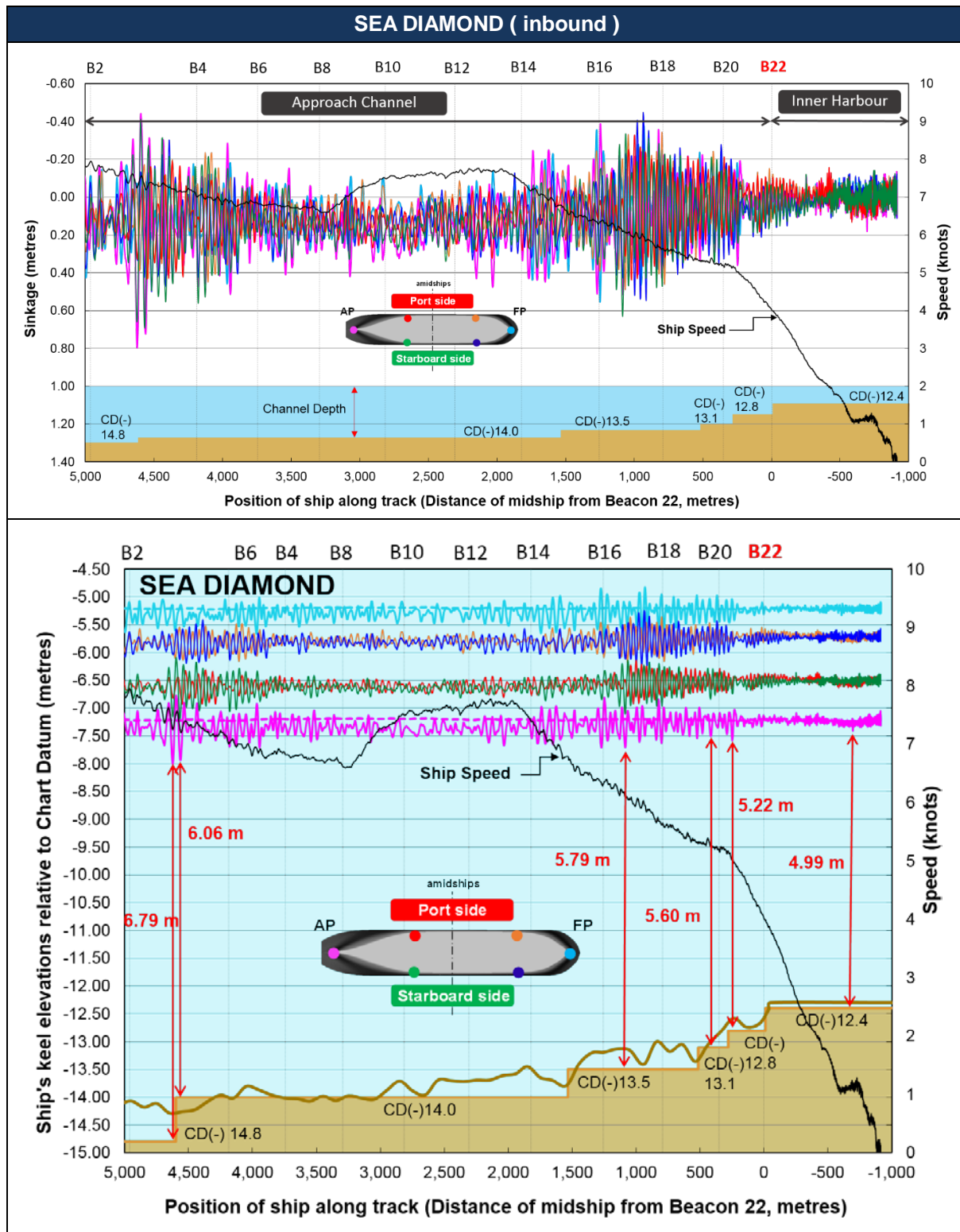
<Top> Measured sinkage (positive downward) at six points. Chart datum depths (not to scale) also shown.

<Bottom> Elevation of the ship's keel relative to chart datum. Broken lines are elevations of the FP and AP including changes in tide only, i.e. their static position, not including squat and wave-induced motions. A flat seabed line is based on the charted depth on AUS 81, and a fluctuating seabed line is the actual survey line provided by OMC International.



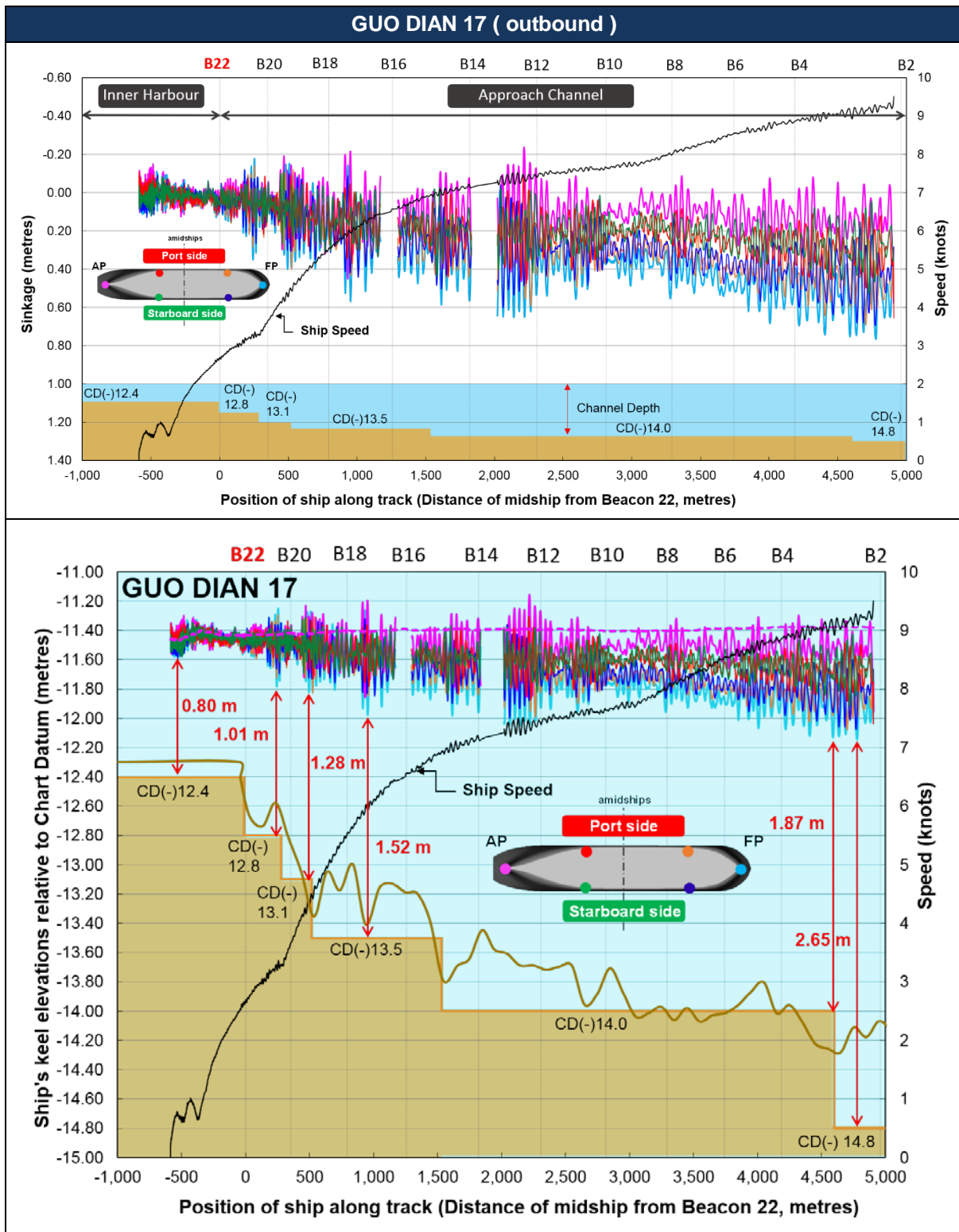
<Top> Measured sinkage (positive downward) at six points. Chart datum depths (not to scale) also shown.

<Bottom> Elevation of the ship's keel relative to chart datum. Broken lines are elevations of the FP and AP including changes in tide only, i.e. their static position, not including squat and wave-induced motions. A flat seabed line is based on the charted depth on AUS 81, and a fluctuating seabed line is the actual survey line provided by OMC International.



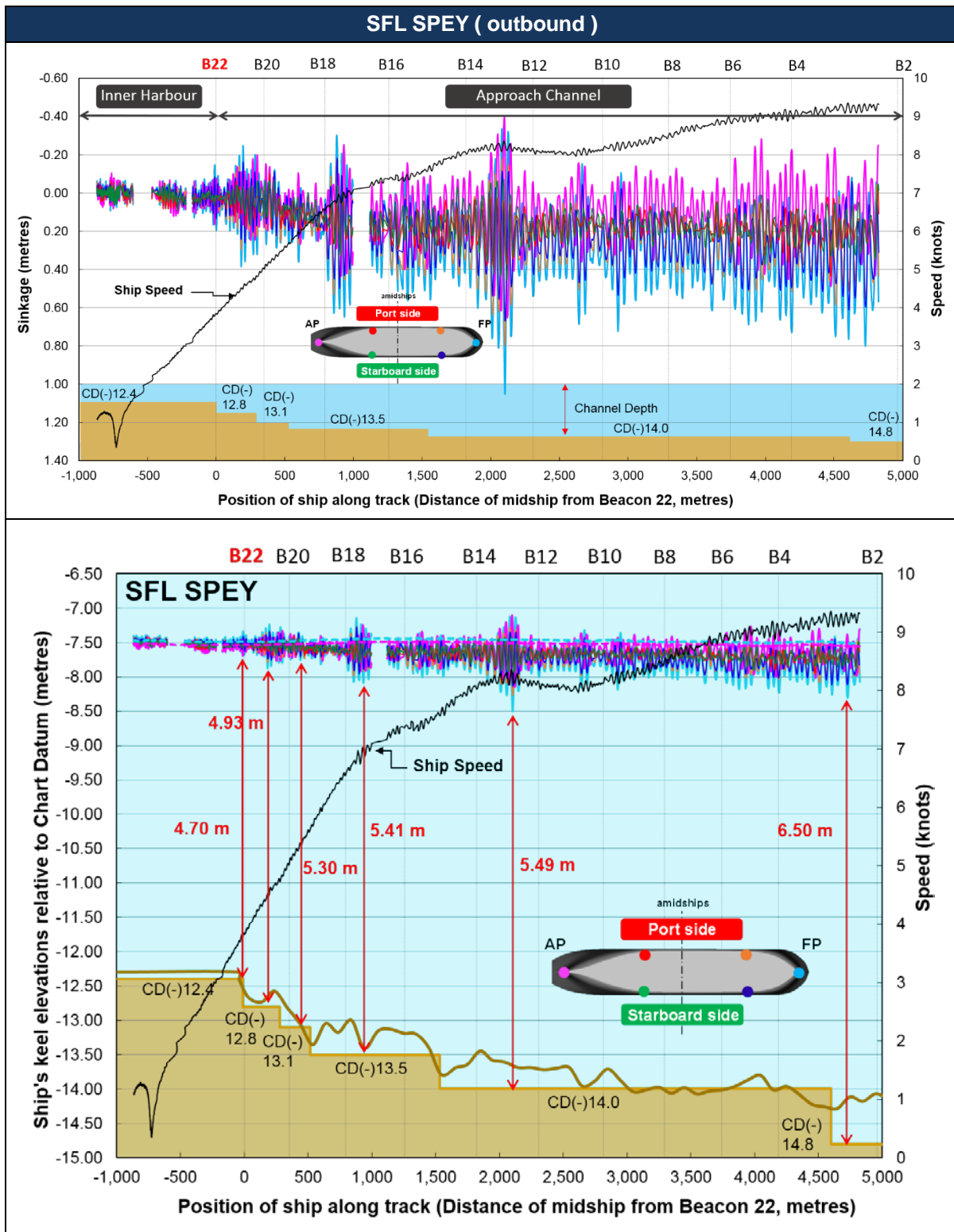
<Top> Measured sinkage (positive downward) at six points. Chart datum depths (not to scale) also shown.

<Bottom> Elevation of the ship's keel relative to chart datum. Broken lines are elevations of the FP and AP including changes in tide only, i.e. their static position, not including squat and wave-induced motions. A flat seabed line is based on the charted depth on AUS 81, and a fluctuating seabed line is the actual survey line provided by OMC International.



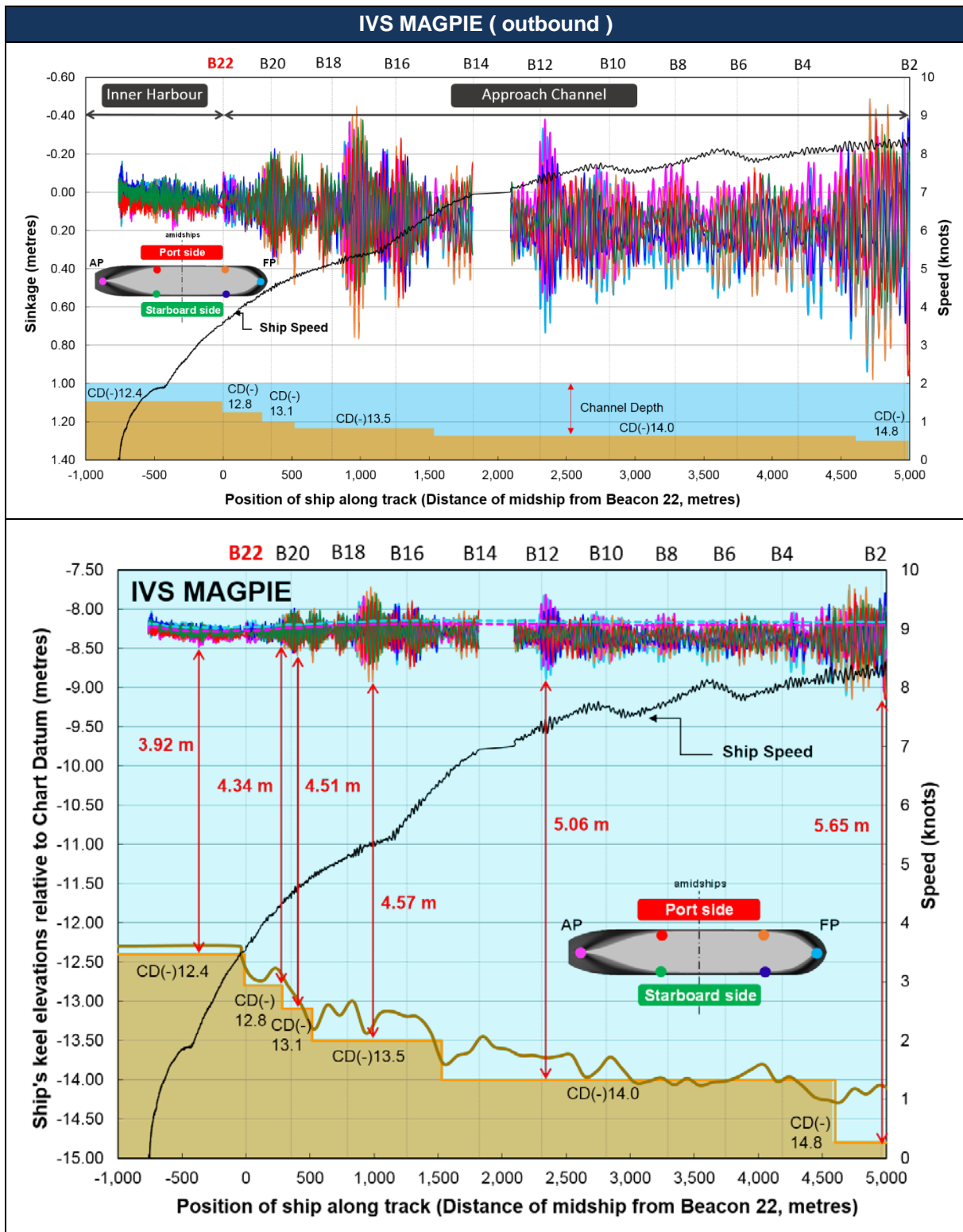
<Top> Measured sinkage (positive downward) at six points. Chart datum depths (not to scale) also shown.

<Bottom> Elevation of the ship's keel relative to chart datum. Broken lines are elevations of the FP and AP including changes in tide only, i.e. their static position, not including squat and wave-induced motions. A flat seabed line is based on the charted depth on AUS 81, and a fluctuating seabed line is the actual survey line provided by OMC International.



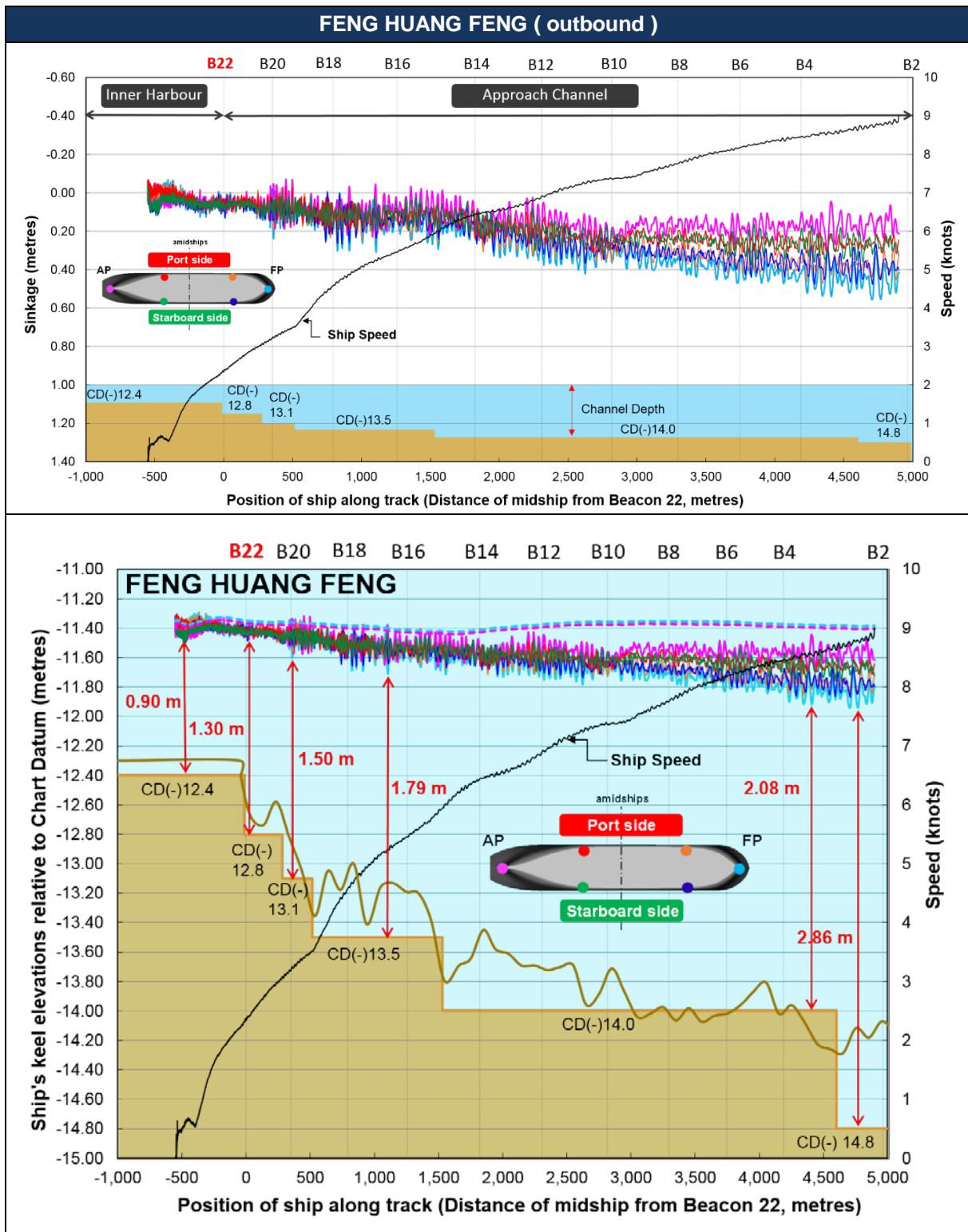
<Top> Measured sinkage (positive downward) at six points. Chart datum depths (not to scale) also shown.

<Bottom> Elevation of the ship's keel relative to chart datum. Broken lines are elevations of the FP and AP including changes in tide only, i.e. their static position, not including squat and wave-induced motions. A flat seabed line is based on the charted depth on AUS 81, and a fluctuating seabed line is the actual survey line provided by OMC International.



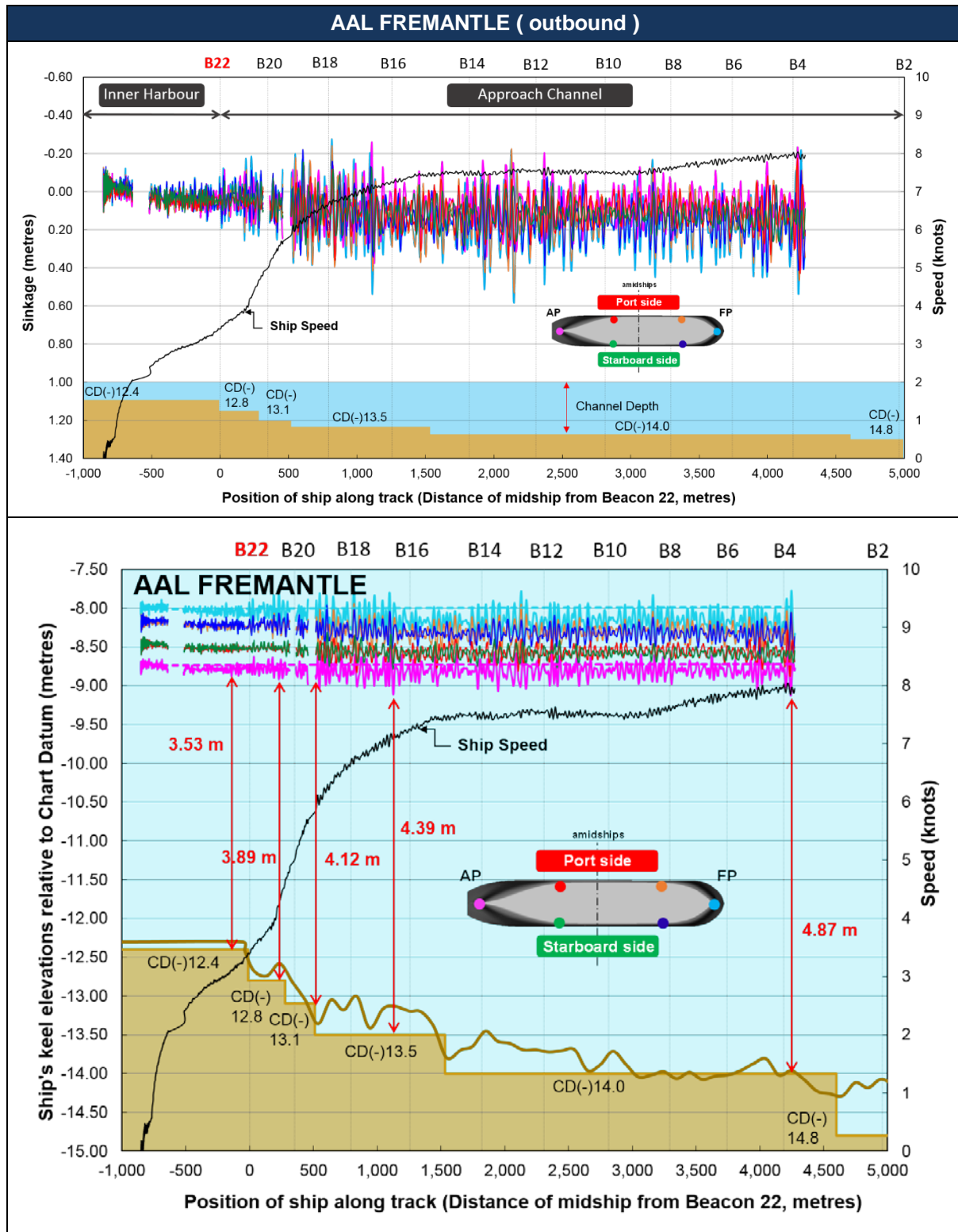
<Top> Measured sinkage (positive downward) at six points. Chart datum depths (not to scale) also shown.

<Bottom> Elevation of the ship's keel relative to chart datum. Broken lines are elevations of the FP and AP including changes in tide only, i.e. their static position, not including squat and wave-induced motions. A flat seabed line is based on the charted depth on AUS 81, and a fluctuating seabed line is the actual survey line provided by OMC International.



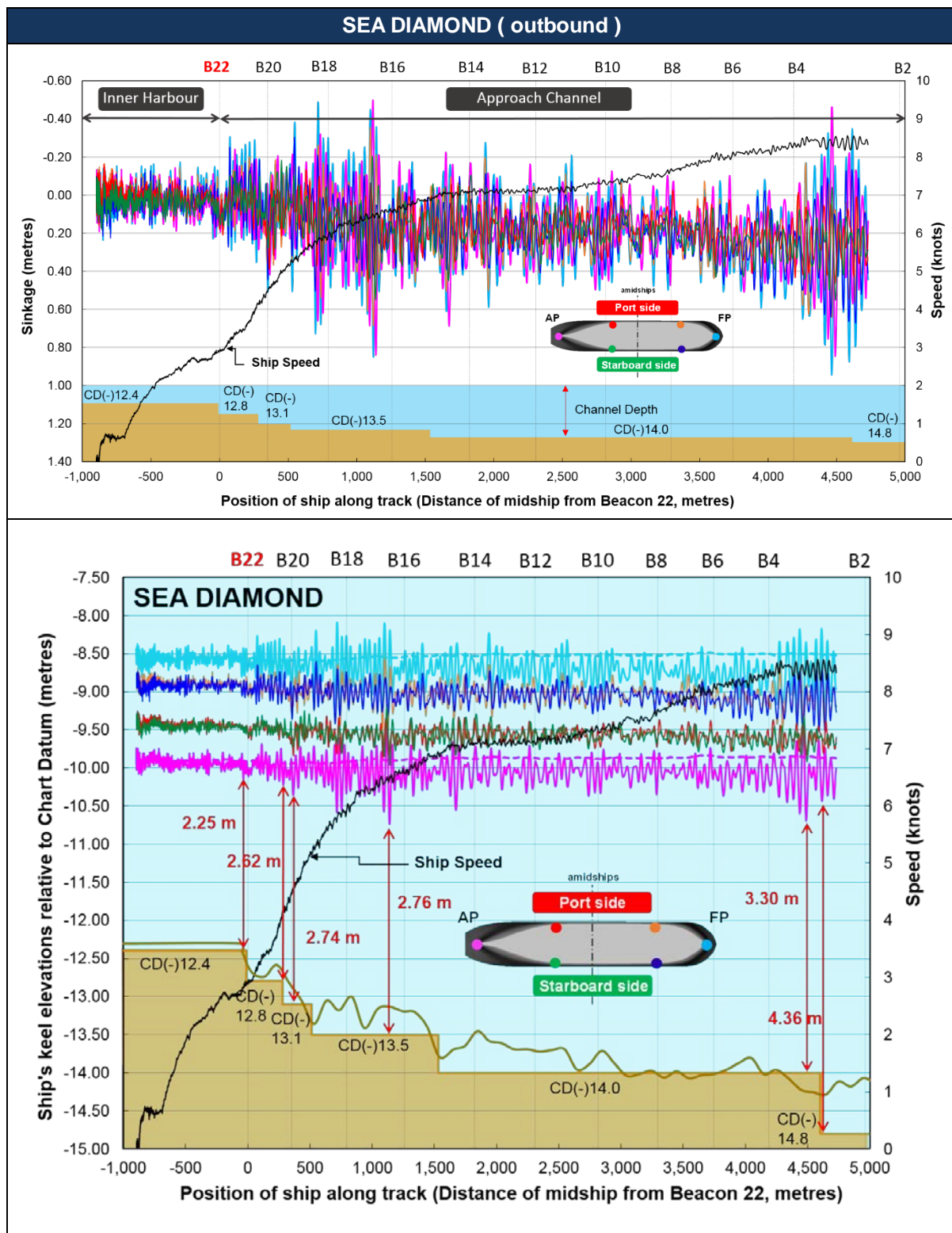
<Top> Measured sinkage (positive downward) at six points. Chart datum depths (not to scale) also shown.

<Bottom> Elevation of the ship's keel relative to chart datum. Broken lines are elevations of the FP and AP including changes in tide only, i.e. their static position, not including squat and wave-induced motions. A flat seabed line is based on the charted depth on AUS 81, and a fluctuating seabed line is the actual survey line provided by OMC International.



<Top> Measured sinkage (positive downward) at six points. Chart datum depths (not to scale) also shown.

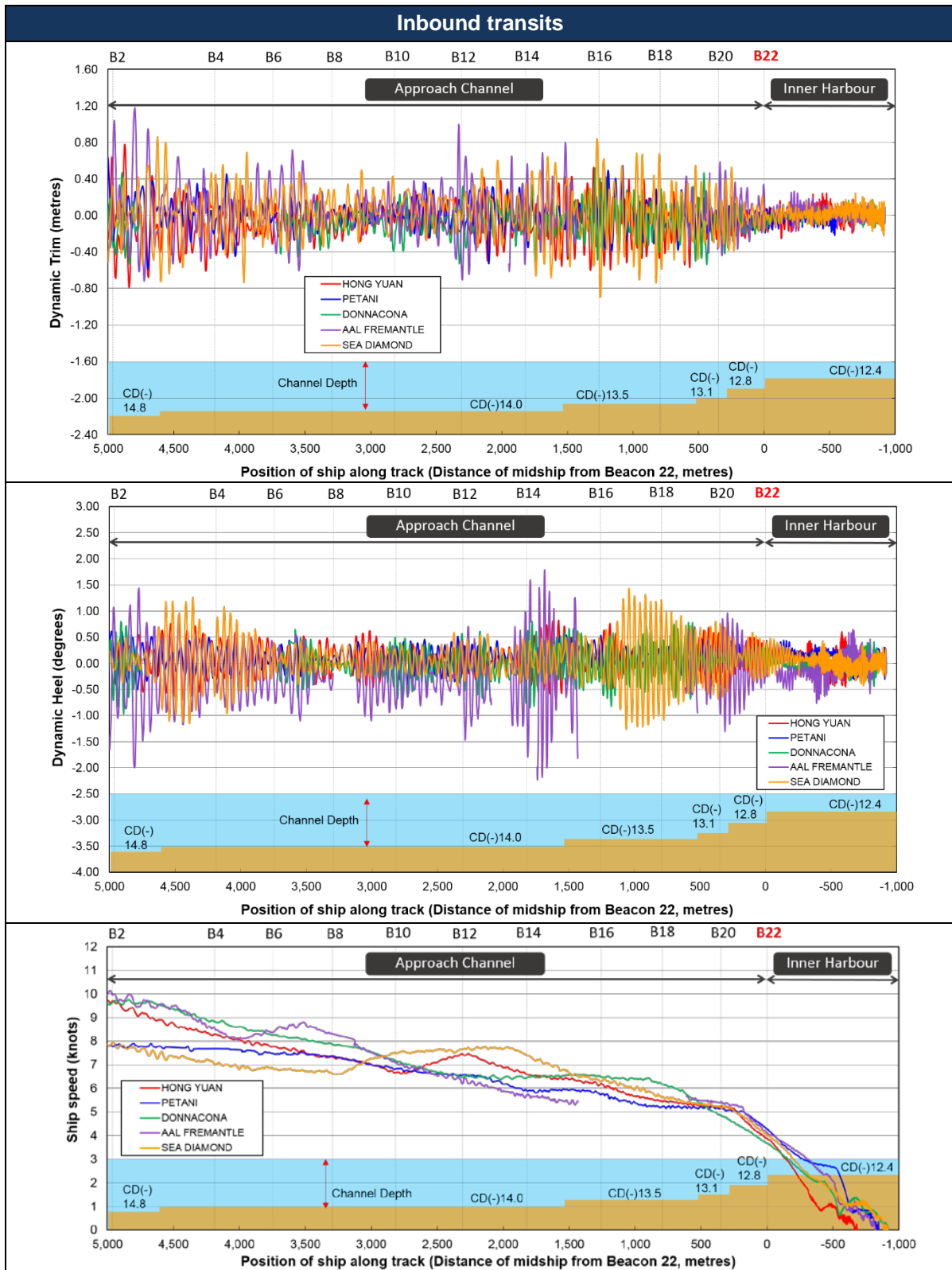
<Bottom> Elevation of the ship's keel relative to chart datum. Broken lines are elevations of the FP and AP including changes in tide only, i.e. their static position, not including squat and wave-induced motions. A flat seabed line is based on the charted depth on AUS 81, and a fluctuating seabed line is the actual survey line provided by OMC International.



<Top> Measured sinkage (positive downward) at six points. Chart datum depths (not to scale) also shown.

<Bottom> Elevation of the ship's keel relative to chart datum. Broken lines are elevations of the FP and AP including changes in tide only, i.e. their static position, not including squat and wave-induced motions. A flat seabed line is based on the charted depth on AUS 81, and a fluctuating seabed line is the actual survey line provided by OMC International.

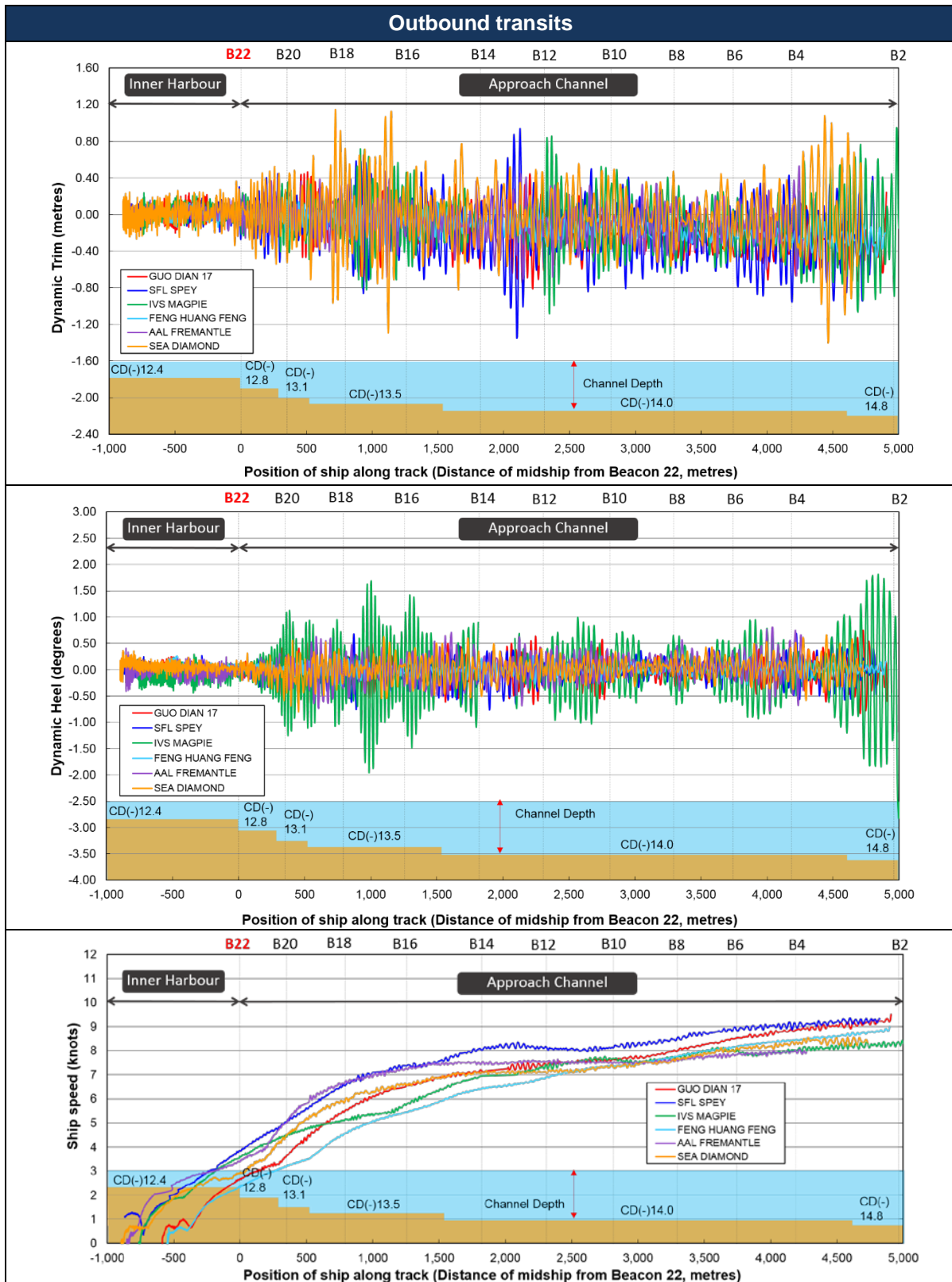
Appendix E – Measured dynamic trim and heel (Graphical results)



<Top> Measured dynamic trim (positive stern-down). Chart datum depths (not to scale) also shown.

<Middle> Measured dynamic heel (positive to starboard). Chart datum depths (not to scale) also shown.

<Bottom> Measured ship speed. Chart datum depths (not to scale) also shown.



<Top> Measured dynamic trim (positive stern-down). Chart datum depths (not to scale) also shown.

<Middle> Measured dynamic heel (positive to starboard). Chart datum depths (not to scale) also shown.

<Bottom> Measured ship speed. Chart datum depths (not to scale) also shown.

Appendix F – Published paper

Ha, J.H., Gourlay, T.P., Nadarajah, N. 2016 Measured ship motions in Port of Geraldton approach channel. *Proceedings, 4th International Conference on Ship Manoeuvring in Shallow and Confined Water, MASHCON 2016*, May 23-25, Hamburg, Germany.

MEASURED SHIP MOTIONS IN PORT OF GERALDTON APPROACH CHANNEL

J H Ha and **T P Gourlay**, Centre for Marine Science and Technology, Curtin University, Australia
N Nadarajah, Global Navigation Satellite Systems Research Centre, Curtin University, Australia

SUMMARY

This article presents some results from a series of recent full-scale trials on measuring dynamic sinkage, trim and heel of 11 bulk carriers entering and leaving the Port of Geraldton. Measurements were carried out using high-accuracy GNSS receivers and a fixed reference station. Measured dynamic sinkage, trim and heel of three example bulk carriers are discussed in detail. A theoretical method using slender-body shallow-water theory is applied to predict the sinkage and trim of the transits. A comparison between measured and predicted results is made to validate the ship motion software for UKC (under-keel clearance) prediction. It is shown that slender-body theory is able to give good predictions of dynamic sinkage and trim. The measured results will also be in future for validating wave-induced motions software.

NOMENCLATURE

AP	After Perpendicular
$AWAC$	Acoustic Wave And Current Profiler
$AWST$	Australian Western Standard Time
B	Ship's beam (m)
C_B	Block coefficient (-)
CD	Chart Datum
C_{s_bow}	Bow sinkage coefficient (-)
C_{s_mid}	Midship sinkage coefficient (-)
C_{s_stern}	Stern sinkage coefficient (-)
C_θ	Trim coefficient (-)
F_h	Depth-based Froude number (-)
FP	Forward Perpendicular
FS	Free Surface
G	GNSS height measurement
g	Acceleration due to gravity (m/s^2)
GM_f	Metacentric height (m), corrected for free surface effect
$GNSS$	Global Navigation Satellite System
GPS	Global Positioning System
h	Water depth (m)
H_s	Significant wave height (m)
HAT	Highest Astronomical Tide
KG	Height of the ship's centre of gravity above keel (m)
LAT	Lowest Astronomical Tide
LCB	Longitudinal centre of buoyancy (m)
LOA	Ship length overall (m)
L_{PP}	Ship length between perpendiculars (m)
MSL	Mean Sea Level
N	Geoid undulations (m)
S_{bow}	Bow sinkage (m)
S_{mid}	Midship sinkage (m)
S_{stern}	Stern sinkage (m)
T	Instantaneous tide height (m)
Θ	Stern-down change in trim due to squat (radians)
T_m	Mean period of the energy spectrum (s)
T_p	Peak period of the energy spectrum (s)
T_ϕ	Ship's natural roll period (s)
U	Ship speed (m/s)
UKC	Under-Keel Clearance
∇	Ship volume displacement (m^3)

1 INTRODUCTION

Safe under-keel clearance (UKC) management is a critical factor in port marine operations and the shipping industry. Accurate guidelines for the optimized UKC could bring the efficient running of the port as well as safety management. The progressively increasing accuracy of GNSS receivers can provide fundamental information for UKC management by allowing full-scale measurements in actual sea conditions.

In September and October 2015, we carried out full-scale trials on some bulk carriers at the Port of Geraldton, located in the mid-west region of Western Australia, in order to measure vertical ship motions relative to still water level including squat and wave-induced motions in its approach channel. Totally 13 ship transits including 2 trials to measure ship motions at a berth have been measured. Measurements were made using the shore-based receiver method that needs to set up high-accuracy GNSS (or GPS) receivers onboard as well as a fixed base station for an external reference [1], [2].

By comparing the vertical motions of a ship when under way to that at berth, considering the changing tide height and geoid undulations, dynamic sinkage, trim and heel are calculated, as well as wave-induced heave, pitch and roll through the entire transit. The dynamic draught at each point on the ship can then be found using those dynamic results and its static draught. UKC in approach channels is also calculated by comparing elevations of the keel of the vessel relative to the seabed. The largest draught over all of the hull extremities governs the net UKC and hence grounding risk.

With high-quality data for the ship motions and environmental conditions, validation of numerical ship motion modelling may also be achieved at full-scale.

2 DESCRIPTION OF THE TRIALS

At the Port of the Geraldton, full-scale trials were performed on 11 inbound and outbound bulk carriers via its curved approach channel (see chart AUS81). The procedure for inbound transits is:

- CMST researchers board vessel with pilot and report to Captain on bridge
- Set up GNSS receivers on bow and both port and starboard bridge wings (symmetric positions)
- Data recording throughout pilotage
- Remove equipment and disembark with pilot

The procedure for outbound transits is the reverse of the above. Data recording covers a period of time before departure or after arrival to take a stationary reading at the berth. In our trials, data recording was commenced prior to leaving the berth for the outbound transits and continued until after all mooring work had been completed for the inbound transits. These are then used as a reference value for comparing the vertical height measurements while under way [2].

Three Trimble R10 GNSS receivers were positioned on the bow extremity centreline, and the port and starboard bridge wings for the measurements. A fixed reference station (Trimble R10 GNSS) was located on the pilot wharf to apply differential corrections to the moving receiver results. This shore-based receiver method is described in [1]. The equipment setup yields 10mm horizontal accuracy and 20mm vertical accuracy in the ship motions. All data were recorded at 1.0 Hz. A typical GNSS receivers setup at the Port of Geraldton is shown in Figure 1.

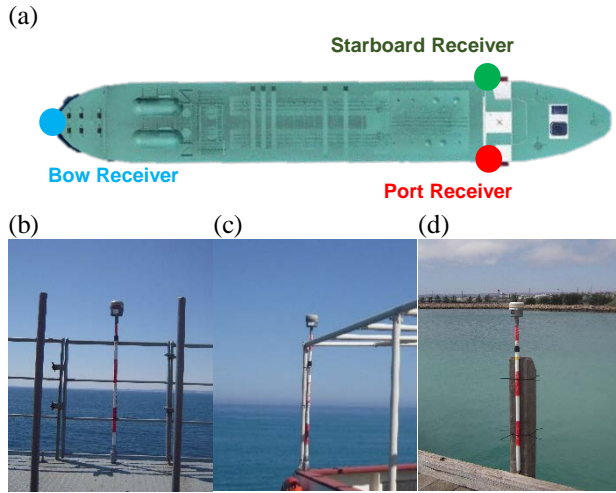


Figure 1. GNSS receivers setup. (a) Plan view of ship receivers. (b) Bow receiver. (c) Port receiver on bridge wing. (d) Base station on pilot wharf.

3 SHIPS AND SHIP TRANSITS ANALYSED IN THIS PAPER

Three transits have been selected for analysis. Table 1 reports pertinent details of these ships that include: *GUO DIAN 17*, built in 2013, a 76,000 DWT Panamax bulk carrier; *FENG HUANG FENG*, built in 2011, a 75,000 DWT Panamax bulk carrier; and *SEA DIAMOND*, built in 2007, a 77,000 DWT Panamax bulk carrier. They each have similar hull dimensions as well as high block coefficient.

Table 1. Details of the ships used for the trials

Particulars	GUO DIAN 17	FENG HUANG FENG	SEA DIA- MOND
L_{OA}	225.00 m	225.00 m	224.99 m
L_{PP}	219.00 m	217.00 m	217.00 m
Beam	32.26 m	32.26 m	32.26 m
Summer draught	14.200 m	14.221 m	14.078 m
Displacement	89,800.8 t	88,535.9 t	87,782.0 t
C_B	0.873	0.868	0.869

Displacement and Block coefficient (C_B) are figures at summer draught. C_B is the ratio of displaced volume to ($L_{PP} \cdot \text{Beam} \cdot \text{Draught}$).

Since each ship may sail under vastly different conditions, we shall take into account all the available relevant operation conditions. Comparative transit conditions for all the ships are shown in Table 2. Details for *GUO DIAN 17* and *FENG HUANG FENG* are based on the data from “Application for Berth” submitted to the Port of Geraldton no later than 2 hours prior to actual departure. For *SEA DIAMOND*, a loading condition report was provided by the shipping agent when CMST researchers disembarked after the measurements. Hydrostatic data was obtained from the Trim and Stability Book for *FENG HUANG FENG* and *SEA DIAMOND*. From the details, we can see that *GUO DIAN 17* and *FENG HUANG FENG* have nearly fully-loaded draught with almost level static trim while *SEA DIAMOND* has a comparatively shallower draught and is trimmed by the stern at departure time. Note that all of these transits are outbound cases.

Table 2. Details of the transit conditions

Particulars	GUO DIAN 17	FENG HUANG FENG	SEA DIA- MOND
Date and Time	28/09/15 09:18~10:13	29/09/15 21:41~22:53	02/10/15 09:52~10:58
Direction	Outbound	Outbound	Outbound
Draught fwd	12.15 m	12.18 m	8.91 m
Draught aft	12.15 m	12.20 m	10.26 m
Departure displacement	75,571 t	74,788 t	57,427 t
C_B	0.859 @12.15m	0.854 @12.20m	0.835 @9.59m
LCB	-	113.9 m @12.20m	115.05 m @9.59m
KG	5.902 m	6.410 m	8.070 m
GM_f	7.109 m	7.100 m	5.930 m

C_B is calculated based on departure draught. LCB is given as metres forward of Aft Perpendicular (AP). For *SEA DIAMOND*, average draught of 9.59m is represented for both C_B and LCB.

Figure 2 shows the Port of Geraldton and its approach channel and beacons together with tracks of the three ships. The channel is around 2.8 nautical miles in length and 180m in width (at toe of bottom slope), varying in depth from 12.4m to 14.8m based on the Chart Datum, which is approximately the level of LAT (Lowest Astronomical Tide). An additional depth of up to 1.2 m can be considered by tides, i.e. HAT (Highest Astronomical Tide) and MSL (Mean Sea Level) in the Port of Geraldton are 1.2 and 0.6m respectively (see chart AUS81). For the outbound ships, the measurements were made from the berth until the ships passed the last beacons (Beacon 1 & 2) at the end of the channel.

Since Geraldton is exposed to long-period swells, which cause wave-induced motions of ships in the channel, measured dynamic sinkage includes wave-induced heave, pitch and roll by the swells. During the trials, waves were measured by an AWAC at Beacon 2 (Latitude 28° 45' 28.2" E, Longitude 114° 33' 55.9" S) and by pressure sensors at Beacon 1, Beacon 3, Beacon 5, ..., Beacon 19.

Wave data from the AWAC at Beacon 2 is shown in Table 3. The full measured wave data will be used to study wave attenuation along the channel, and wave-induced motions along the channel, in future work.

Table 3. Measured wave data at Beacon 2 during the transits

Transits	AWST	Hs (m)	Tp (sec)	Tm (sec)	Dir (deg)
GUO DIAN 17	28/09/15 09:18	1.49	13.3	8.8	247
	28/09/15 09:38	1.22	12.5	8.2	242
	28/09/15 09:58	1.29	9.2	8.2	244
	28/09/15 10:18	1.12	13.0	7.8	243
FENG HUANG FENG	29/09/15 21:38	0.57	10.8	6.7	240
	29/09/15 21:58	0.55	12.2	6.5	248
	29/09/15 22:18	0.53	12.3	6.4	248
	29/09/15 22:38	0.53	12.5	6.8	251
	29/09/15 22:58	0.52	11.8	6.6	240
SEA DIA- MOND	02/10/15 09:58	1.83	13.8	12.1	245
	02/10/15 10:18	1.56	13.8	11.5	246
	02/10/15 10:38	1.51	13.8	11.3	248
	02/10/15 10:58	1.61	15.1	11.5	252

The time of each record is the time at the end of the 20 minutes in which the data was recorded.

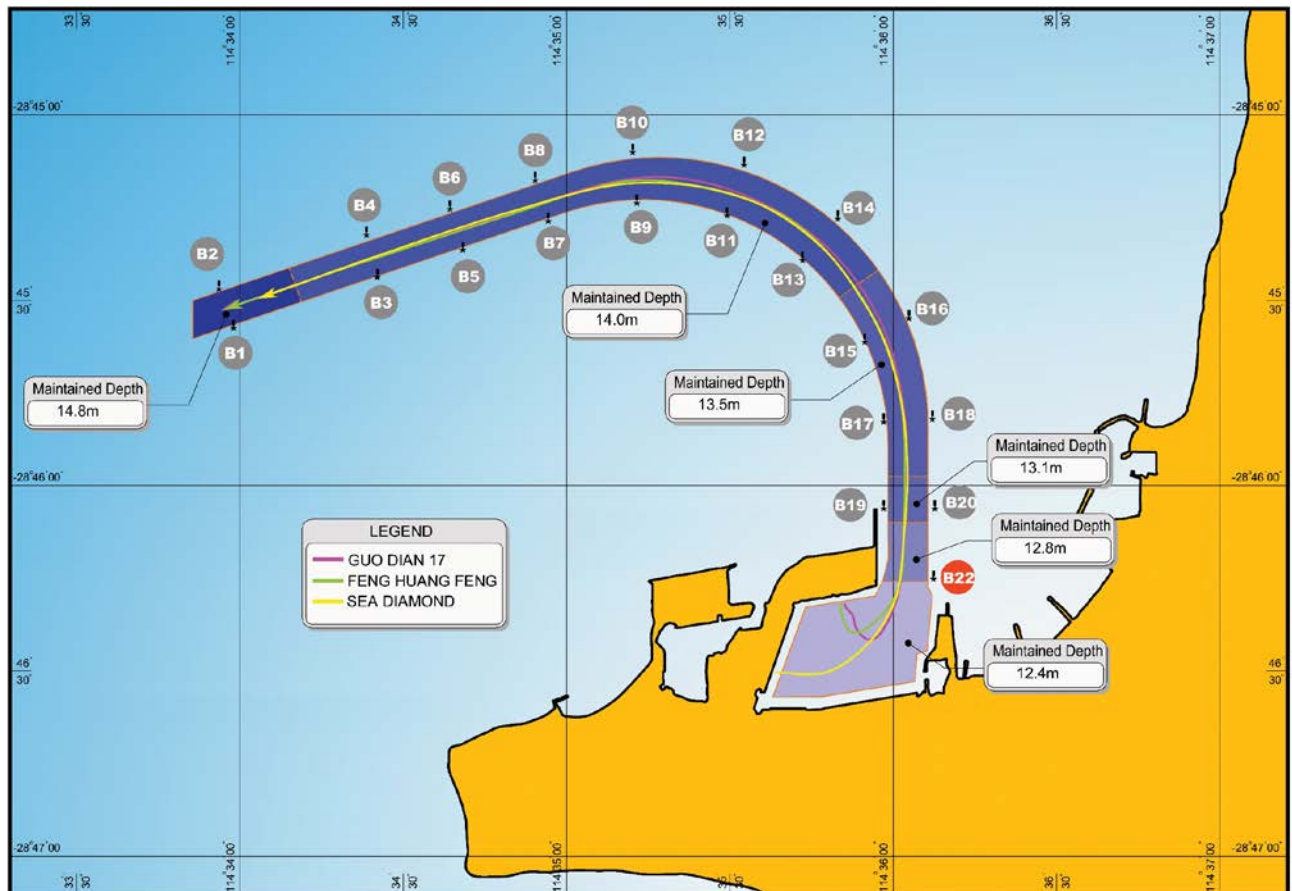


Figure 2. Port of Geraldton approach channel and measured midship tracks.

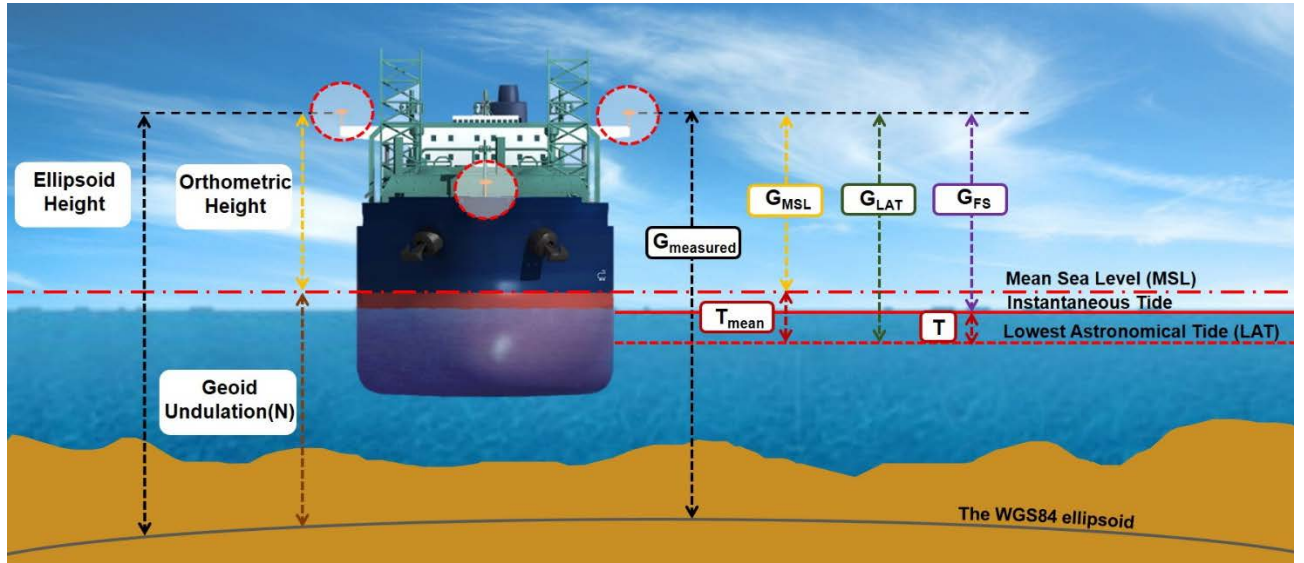


Figure 3. Components for calculating sinkage from GNSS height measurements.

By accurately measuring the vertical elevations of the three GNSS receivers on each ship with respect to the local static waterline, and assuming the ship to be rigid, sinkage at each point of concern of running aground on the ship can be calculated, as well as dynamic trim and dynamic heel. Dynamic heel is here defined as the change in heel angle relative to the static floating position [3], and sinkage is defined as being positive downward.

Figure 3 shows height components for calculating sinkage from GNSS height measurements, and equation (1) is given for their relationship. This method for sinkage calculation is presented in [1], [2].

$$\text{Sinkage} = (G_{\text{measured}} - N + T_{\text{mean}} - T)_{\text{static}} - (G_{\text{measured}} - N + T_{\text{mean}} - T)_{\text{underway}} \quad (1)$$

Regarding tidal data, local tide has been extracted from the data that is raw sea surface elevations as measured at Berth 3-4 in the Port of Geraldton, using a low pass filter with a cutoff frequency of 5 minutes.

4.1 DYNAMIC SINKAGE

It would be more effective to see measured vertical motions of the ship against the same horizontal axis that uses cumulative distance from a fixed point for all the ships. The pilots normally state their position in the channel using the beacons, so we use Beacon 22 as the fixed point as marked with a red circle in Figure 2. The horizontal axis is, hence, described as distance out from Beacon 22 in metres and has vertical lines at locations of Beacon 20, Beacon 18, ..., Beacon 2 (hereafter referred to as B). Distance within the harbour, therefore, is negative. Note that substantial gaps in the data of GUO DIAN 17 around B16 and B14 are due to GPS fixes being of insufficient quality and being rejected.

Measured sinkage results together with corresponding ship speed profile, as well as the bathymetry along the channel, are shown in Figure 4. With positions of the FP and AP, the forward and aft shoulder of the bilge corners are also plotted as they can be specifically vulnerable to grounding considering the combined effects of dynamic trim and heel and the ships' long parallel midbodies. A parallel body line from the Deck and Profile drawing for SEA DIAMOND is used for the positions of the forward and aft shoulders of the bilge corners, approximately 75.3% and 36.0% of L_{PP} forward of Aft Perpendicular (AP) respectively. These proportions are also applied to those for GUO DIAN 17 and FENG HUANG FENG.

Distance of 89%, 91% and 88% of the half-beam away from the centerline of the ships have been taken for the transversal positions of the bilge corners from the sections of the General Arrangement Plan for GUO DIAN 17, FENG HUANG FENG and SEA DIAMOND respectively. An estimated 90% of that is hence applied to the ships uniformly.

Dynamic sinkage includes a near-steady component due to the Bernoulli Effect at forward speed, which is characterized by a bodily sinkage and a dynamic change in trim. This effect is known as squat, and can be predicted with theoretical or empirical methods. As well as this, the sinkage has oscillations due to wave-induced motions. When swell waves are present, vertical motions of the ship are more intricate with its wave-induced motion that is a combination of heaving, pitching and rolling. For example, the SEA DIAMOND transit was undertaken in large, long period swell conditions (Table 3), and vertical motions are seen to be highly oscillatory (Figure 4) due to wave-induced heave, pitch and roll.

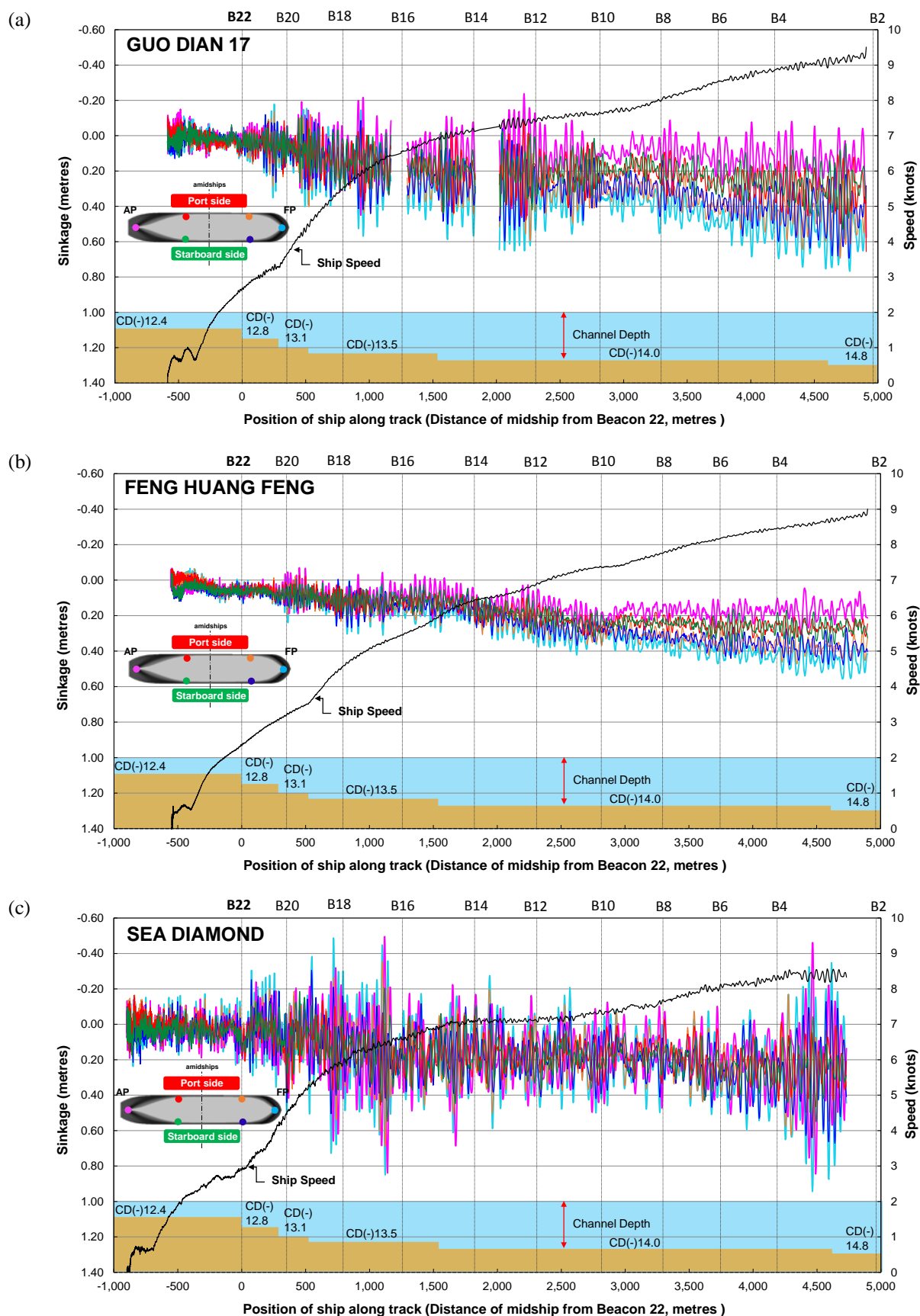


Figure 4. Measured sinkage (positive downward) at six points for (a) GUO DIAN 17, (b) FENG HUANG FENG and (c) SEA DIAMOND. Chart datum depths (not to scale) also shown.

Based on Chart AUS81, outbound transits are on a heading of 0° (North) from B20 to B18, then an approximate 1,200m-radius turn to port, steadying on a heading of 251° from B8 to the end of the channel. By comparing this to directions of the prevailing swells in Table 3, we see that the ships were in port beam seas near B18 and in head seas near B4.

Maximum sinkage is observed at the bow in the vicinity of B2, i.e. near the end of the channel, but significant oscillations also occurred when they are travelling between B20 and B12. This is common to all the ships and might be referable to combined effect of dynamic trim and heel changes due to turning manoeuvres and beam waves in this severely curved section. The maximum sinkage is: 0.77m (0.35% of L_{PP}) for GUO DIAN 17; 0.56m (0.26% of L_{PP}) for FENG HUANG FENG; and 0.94m (0.44% of L_{PP}) for SEA DIAMOND.

With swell present, maximum dynamic draught may occur at the forward shoulders of the bilge corners [4]. This is evidenced by looking at the sinkage at the forward shoulders of the bilge corners that had a greater sinkage than the bow at some instants in the cases of the GUO DIAN 17 and SEA DIAMOND transits. However, with considering the fact that SEA DIAMOND used the static stern-down trim of 1.35m on her departure (see Table 2), the stern still has the maximum dynamic draught (refer to the Appendix). No significant wave-induced heave, pitch and roll in the FENG HUANG FENG transit were seen with calm wind and low swell conditions.

In order to bring further practical support to UKC management in the port, the ship's vertical motions should be addressed with elevations of the ship's keel relative to Chart Datum so that the port may know the actual real-time clearance from the seabed. An Appendix is made to include these vertical elevation changes. The minimum real-time clearance of 0.80, 0.90 and 2.25m is captured for

GUO DIAN 17, FENG HUANG FENG and SEA DIAMOND respectively.

The starboard forward shoulder of the bilge corners for GUO DIAN 17 and the starboard aft shoulder of the bilge corners for FENG HUANG FENG are the closest points to the seabed over their entire transits. These closest points are observed in the harbour, and this is primarily due to heel, as tugs pulled the ships to starboard during unberthing. For SEA DIAMOND with having the static stern-down trim, the AP is the point closest to the seabed through the whole transit.

In the appendix, elevations of the FP and AP including changes in tide only, i.e. their static position, not including squat and wave-induced motions, are plotted as broken lines. This shows how much of the sinkage is due to tide changes.

4.2 DYNAMIC TRIM

Bulk carriers with level static trim tend to have dynamic trim by the bow when the ship is under way, see e.g. [5] for model-scale test results, [6] for full-scale test results. This large bow-down trim means that the bow can be the point on the ship most vulnerable to grounding. Figure 5 shows results of dynamic trim for the three transits. Steadily increasing trim by the bow is observed for all the three cases, but is swamped by wave-induced pitching for SEA DIAMOND. Note that dynamic trim is given in metres based on the difference between the FP and AP.

By looking at oscillations of dynamic sinkage (see Figure 4) for each transit, it is identified that dynamic trim is more likely to affect maximum sinkage for bulk carriers rather than dynamic heel which will be discussed subsequently. This situation is different to container ships, where dynamic heel may be the most important factor governing maximum sinkage [2].

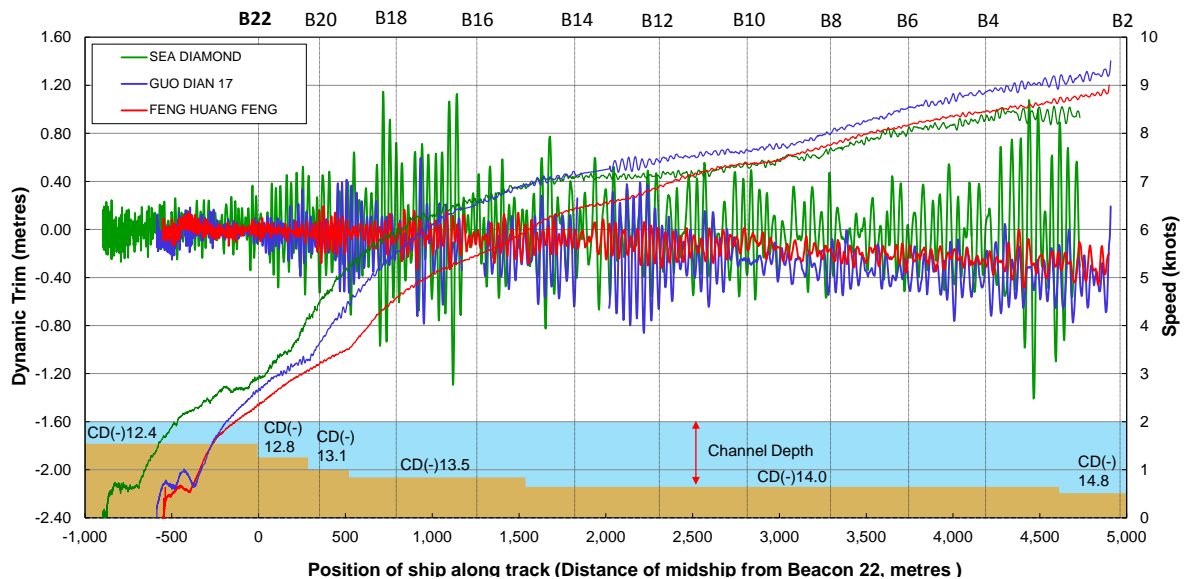


Figure 5. Measured dynamic trim (positive stern-down) for the three transits. Chart datum depths (not to scale) also shown.

According to full-scale tests made by [7] and [8], acceleration and deceleration influence dynamic trim. GUO DIAN 17 and SEA DIAMOND quickly accelerate speed up to 6 knots while they pass between B22 and B18. For the SEA DIAMOND case, some significant oscillations in dynamic trim are seen in the regions of near B18, B16 and the end of the channel. This may be explained considering the operation condition with comparatively larger swell (see Table 3, mostly head sea condition) but lighter displacement.

The maximum dynamic trim by the bow are 0.86m, 0.49m and 1.40m (0.39%, 0.23% and 0.65% of the L_{PP}) for the GUO DIAN 17, FENG HUANG FENG and SEA DIAMOND transit respectively.

4.3 DYNAMIC HEEL

Dynamic heel may cause the bilge corners to be the closest points to the seabed. For ports exposed to long-period swell, large dynamic heel occurs when the wave encounter period is close to a ship's natural roll period [9]. The natural roll period T_ϕ is approximately

$$T_\phi = 0.8 \frac{B}{\sqrt{GM_f}} \quad (2)$$

More accurate calculations of the natural roll period and wave-induced motions will be done in future publications. Calculated natural roll periods of the ships measured are shown in Table 4. SEA DIAMOND has smaller GM_f (see Table 2) and hence longer natural roll period.

Table 4. Calculated natural roll period for the trials

Natural roll period	GUO DIAN 17	FENG HUANG FENG	SEA DIAMOND
T_ϕ	9.7 sec	9.7 sec	10.6 sec

By comparing the mean wave period (see Table 3) to the ships' natural roll period, we would expect large roll angles to occur in the GUO DIAN 17 and SEA DIAMOND cases. Measured dynamic heel for the examples are shown in Figure 6. As expected, larger heel oscillations are seen in these cases. Of equal importance is wave height. FENG HUANG FENG travelled in low swell conditions and hence has small roll angles.

An oscillation pattern in dynamic heel between each beacon in the curved section of the channel (between B18 and B10) is equally observed for all the three transits. This repetitive pattern may be partly attributable to rudder-induced heel due to turning manoeuvres. This will be studied further in future work, with reference to the measured rudder changes and calculated wave-induced motions. As mentioned in 4.1, due to tugs for unberthing, considerable heel to starboard is observed in the harbour, i.e. before B22, for all the cases.

Container ships with level static trim generally have significant heel arising from wind and turning in calm water. For example, heel angles in the order 1° to 2° were measured for container ships in Hong Kong [3]. However, bulk carriers have relatively large displacement (for the same ship length), low KG and small above-water profile area, which translated into smaller heel angles due to wind and turning.

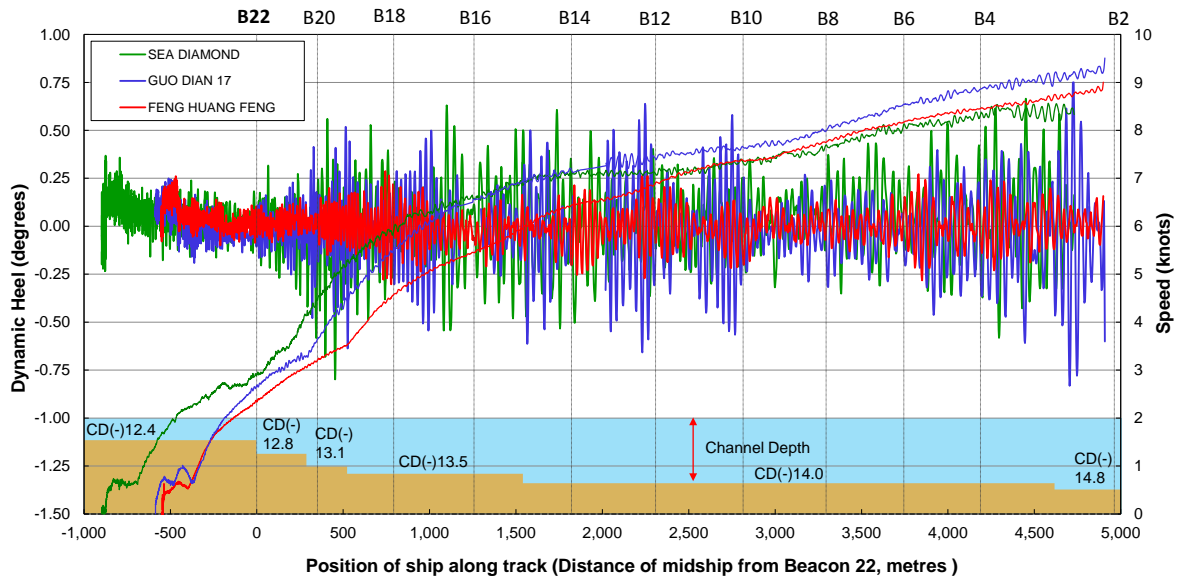


Figure 6. Measured dynamic heel (positive to starboard) for the three ships. Chart datum depths (not to scale) also shown.

5 THEORETICAL SQUAT PREDICTIONS

As Port of Geraldton approach channel is a typically dredged channel in channel dimensions, a differential between channel depth and depths on the side of the channel is observed with bathymetric data on the nautical chart (see chart AUS81), e.g. depths on the side of the channel are around 3m shallower than in the dredged channel in the longest section with a maintained depth of 14.0 m, a conceptual cross section of which is shown in Figure 7.

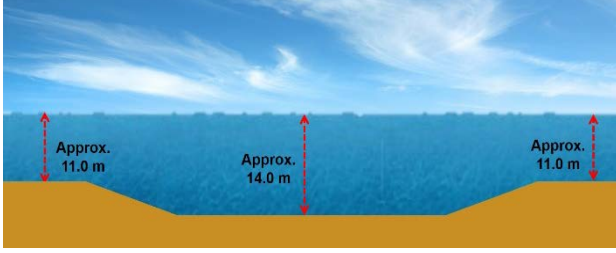


Figure 7. Conceptual cross section of Port of Geraldton approach channel. This view is for illustration only (not to scale).

Some port approach channels in Western Australia including Geraldton have been assessed to see whether a particular ship and channel configuration may be classed as open water, or whether a specific narrow-channel analysis is required. Regarding a Panamax carrier case (L_{PP} 215m), the sinkage coefficient for Geraldton channel has been predicted within 3% of the open-water value using the slender-body theory [10]. For predicting ship sinkage and trim, therefore, the transits can be classed as open water condition since the effect of transverse bathymetries such as channel width and trench depth to the ships having L_{PP} of 217 and 219 m is seen to be minimal.

5.1 TUCK METHOD

A theoretical method used here to compare against the measured ship sinkage and trim is based on slender-body shallow water theory of [11] for open water, modified slightly to make it more applicable to ships with transom sterns, as in [12]. This method uses linearized hull and free-surface boundary conditions. According to that theory, the sinkage at midships (midway of L_{PP}), bow and stern can be written

$$S_{mid} = C_{s_{mid}} \frac{\nabla}{L_{PP}^2} \frac{F_h^2}{\sqrt{1-F_h^2}} \quad (3)$$

$$S_{bow} = C_{s_{bow}} \frac{\nabla}{L_{PP}^2} \frac{F_h^2}{\sqrt{1-F_h^2}} \quad (4)$$

$$S_{stern} = C_{s_{stern}} \frac{\nabla}{L_{PP}^2} \frac{F_h^2}{\sqrt{1-F_h^2}} \quad (5)$$

where F_h is the depth-based Froude number:

$$F_h = \frac{U}{\sqrt{gh}} \quad (6)$$

Similarly, the change in stern-down trim due to squat θ , can be written

$$\theta = C_{\theta} \frac{\nabla}{L_{PP}^3} \frac{F_h^2}{\sqrt{1-F_h^2}} \quad (7)$$

Calculations are done using the slender-body shallow water theory [11], as implemented in the computer programme “ShallowFlow” [13].

5.2 SHIP HULLFORMS MODELLED

Since stability and hydrostatic data were obtained for each ship, but not lines plans or hull offsets, a representative hull that has similar characteristics of the hulls was chosen and modified to match the main hull parameters. For minimum modification, the other dimensionless parameters such as block coefficient (C_B) and longitudinal centre of buoyancy (LCB) should also be reasonably similar.

For the theoretical prediction, FHR ship G, a Panamax bulk carrier hull commissioned by Flanders Hydraulics Research and Ghent University, Belgium [14], [15], has been chosen. Modifications of FHR ship G hull have been made from the supplied IGES file in order to match information on the ships’ Trim and Stability Book, as described in [16].

Figure 8 shows an example of the modelled ship G with the bow, stern, profile and bottom views. We see that ship G hull is very block-like with a long parallel midbody and a smaller transom that are considered typical features of bulk carriers in hull shape.

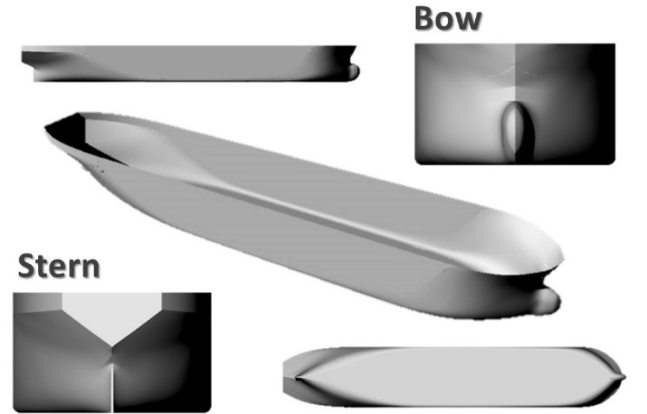


Figure 8. An example of the modelled Ship G.

We have made two kinds of the modified FHR ship G, based on load and ballast conditions for the three ships at the actual departure time. One is applied to SEA DIAMOND, and the other is for both GUO DIAN 17 and FENG HUANG FENG due to the resemblance in transit conditions (see Table 2).

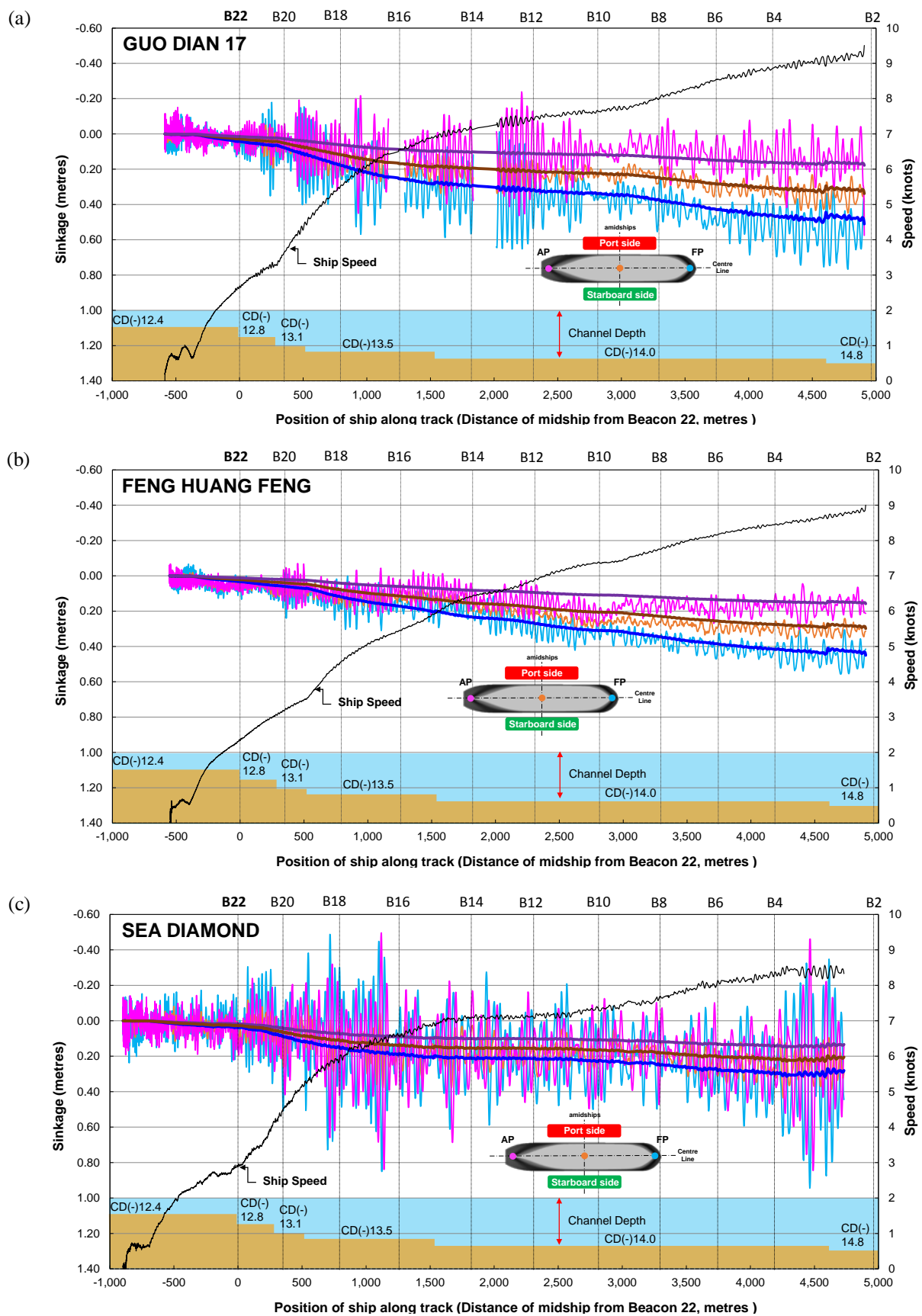


Figure 9. Measured and calculated sinkage (positive downward) at the FP, AP and midship for (a) GUO DIAN 17, (b) FENG HUANG FENG and (c) SEA DIAMOND. Calculations do not include wave-induced motions. Chart datum depths (not to scale) also shown.

5.3 RESULTS

Calculated bow, stern and midship sinkage coefficients for each ship using the slender-body theory of [11] are shown in Table 5. These are then applied to equation (3), (4) and (5) for calculating the theoretical sinkage.

Table 5. Calculated sinkage coefficients for each ship in open water

Sinkage Coefficient (C_s)	GUO DIAN 17	FENG HUANG FENG	SEA DIA-MOND
FP (C_{s_bow})	2.00	1.95	1.82
Midship (C_{s_mid})	1.32	1.29	1.33
AP (C_{s_stern})	0.70	0.68	0.87

Comparisons between measured and predicted sinkage for the FP, AP, and midship for the transits, together with measured ship speed and the bathymetry along the channel, are shown in Figure 9.

It is known that Tuck's method [11] tends to under-predict the sinkage of cargo ships in finite-width canal model tests, especially in very narrow canals [17], [18]. No model tests approximating open-water dredged channels are available with which to compare. In the full-scale trials, given that the transits involve significant speed and depth changes along the channel, the overall performance of the theoretical method is quite good, but the theory [11] is still seen to slightly under-predict the sinkage. For FENG HUANG FENG, midship sinkage predictions are on average 13% less than the measurements for speeds above 7 knots. For GUO DIAN 17 and SEA DIAMOND, midship sinkage also appears to be under-predicted, but the measurements are swamped by wave-induced heave.

Reliability of the measurements is made with a vertical accuracy of 20mm of the equipment [19], but there are additional problems in applying Tuck's theory to the transit conditions, such as: the seabed that cannot be perfectly flat

in the longitudinal or transverse directions; the seabed condition (e.g. mud, sand, rock, sea grass, and corals); the effect of the approximated hull geometry. These factors all could make application of the theory complicated.

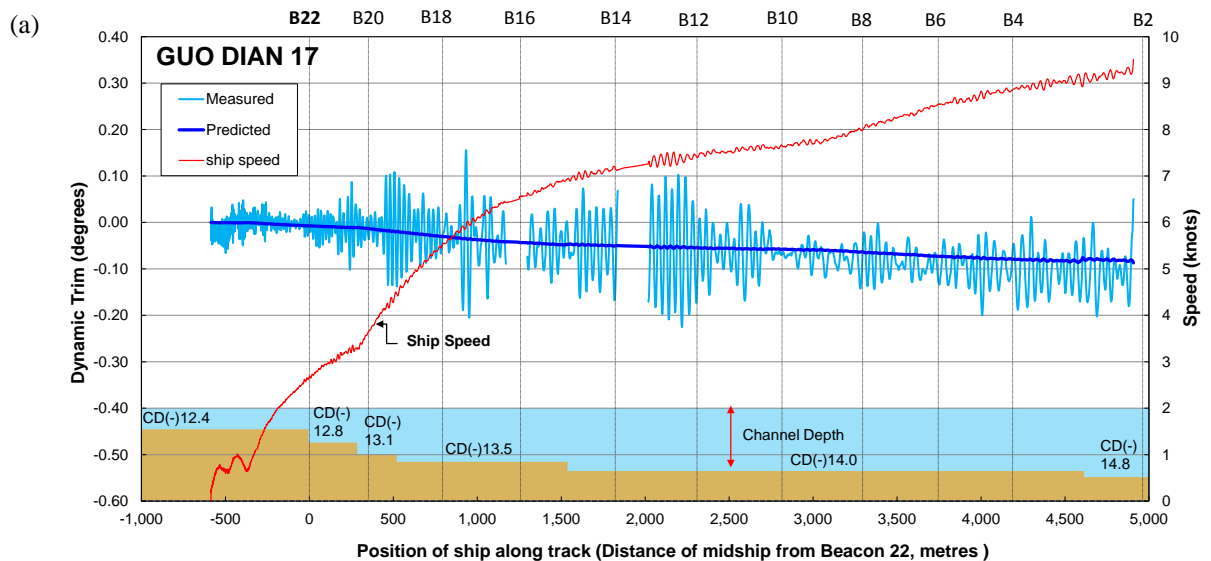
Table 6 lists the theoretical trim coefficients for each ship using equation (7). This is also applied for calculating the theoretical change in stern-down trim due to squat θ . All three transits have negative trim coefficients, indicating negative (bow-down) dynamic trim.

Table 6. Calculated trim coefficients for each ship in open water

Trim Coefficient	GUO DIAN 17	FENG HUANG FENG	SEA DIA-MOND
C_θ	- 1.30	- 1.27	- 0.96

The trim coefficient, and hence dynamic trim, is quite sensitive to hull shape, so complete ship offsets are required to accurately calculate dynamic trim using the slender-body theory [11], [20]. Since such offsets are generally confidential for merchant cargo ships, approximations to the hull shape have been made by modifications of FHR ship G hull, as mentioned in 5.2.

Figure 10 shows comparisons between measured and predicted dynamic trim. Dynamic trim is given here in degrees ($^\circ$).



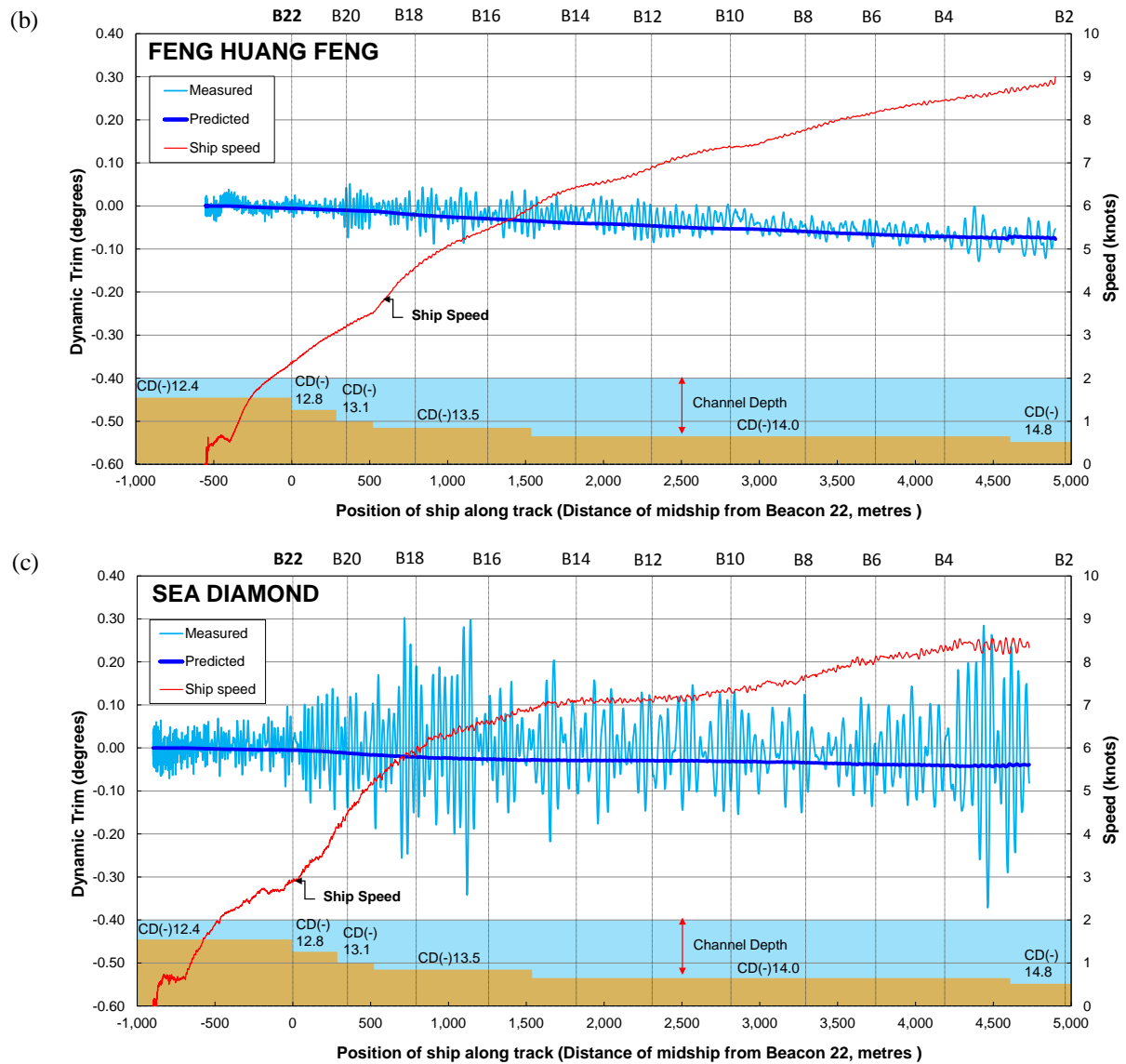


Figure 10. Measured and calculated dynamic trim (positive stern-down) for (a) GUO DIAN 17, (b) FENG HUANG FENG and (c) SEA DIAMOND. Chart datum depths (not to scale) also shown.

Predicted dynamic trim for FENG HUANG FENG and SEA DIAMOND are slightly more bow-down (or less stern-down) than measured whereas GUO DIAN 17 shows a predicted dynamic trim of less bow-down. Considering the above-mentioned approximations, it is found that the theoretical prediction quite closely estimates dynamic trim at full-scale.

6 CONCLUSIONS

For under-keel clearance management, dynamic sinkage, trim and heel of the three outbound bulk carriers have been analysed in detail among a total of 11 measurements in the Port of Geraldton. All measured motion data presented here are from the GNSS receivers with the fixed reference station. The following conclusions are drawn from the study:

- High-quality data have been acquired from the set of full-scale trials
- The trial results will be made publicly-available so that they can be used for validating current UKC practice by ports and as a set of benchmarking data internationally
- Three outbound transits have been chosen for detailed analysis in this paper: a transit in low swell (FENG HUANG FENG); a transit with large swell (SEA DIAMOND) and a transit with medium swell (GUO DIAN 17)
- Maximum sinkage, including the effects of squat and wave-induced motions, occurred at the bow and ranges between 0.26% and 0.44% of L_{PP} for the three ships considered here

- Slender-body theory is able to predict squat (steady sinkage and trim) with reasonable accuracy for bulk carriers at full-scale in open dredged channels. A small empirical correction to the theory is advisable for better UKC prediction

7 ACKNOWLEDGEMENTS

The authors wish to thank all of the marine pilots and staff at Mid West Ports Authority for their assistance, support and enthusiasm in conducting the trials. We would also like to acknowledge the following organizations for their contributions to this research: Tianjin Guodian Shipping, China Shipping Tanker and Hanaro Shipping, who provided access to and hull information for GUO DIAN 17, FENG HUANG FENG and SEA DIAMOND respectively; the GNSS Research Group, Curtin University, who provided the GNSS equipment; Tremarfon Pty Ltd, who provided measured tide and wave data; Flanders Hydraulics Research and Ghent University, who provided hull data for Ship G; and OMC International, who provided surveyed depth data for the channel.

8 REFERENCES

1. Feng, Y.; O'Mahony, S. (1999). Measuring Ship Squat, Trim, and Under-Keel Clearance using On-the-Fly Kinematic GPS Vertical Solutions, *Journal of the Institute of Navigation* 46(2): pp.109-117.
2. Gourlay, T.P.; Klaka, K. (2007). Full-scale measurements of containership sinkage, trim and roll, *Australian Naval Architect* 11(2): pp.30-36.
3. Gourlay, T.P. (2008). Dynamic draught of container ships in shallow water, *International Journal of Maritime Engineering* 150(4): pp.43-56.
4. Gourlay, T.P. (2007). Ship Underkeel Clearance in Waves, *Proceedings of the Coasts & Ports 2007 Conference*, Melbourne, Australia.
5. Dand, I.W.; Ferguson, A.M. (1973). The squat of full form ships in shallow water, *Trans. RINA* 115: pp.237-255.
6. Härting, A.; Laupichler, A.; Reinking, J. (2009). Considerations on the squat of unevenly trimmed ships, *Ocean Engineering* 36(2): pp.193-201.
7. Ferguson, A.M.; McGregor, R.C. (1986). On the Squatting of Ships in Shallow and Restricted Water, *Coastal Engineering Proceedings* 1(20).
8. Hatch, T. (1999). Experience measuring full scale squat of full form vessels at Australian ports, *Proceedings of the Coasts & Ports 1999 Conference*, Perth, Australia.
9. Gourlay, T.P. (2015). Ship under-keel clearance. Navigation Accidents and their Causes, *The Nautical Institute*.
10. Ha, J.H.; Gourlay, T.P. (2015). Bow and Stern Sinkage Coefficients for Cargo Ships in Shallow Open Water, *under review*.
11. Tuck, E.O. (1966). Shallow water flows past slender bodies, *Journal of Fluid Mechanics* 26: pp.81-95.
12. Gourlay, T.P. (2008). Slender-body methods for predicting ship squat, *Ocean Engineering* 35(2): pp.191-200.
13. Gourlay, T.P. (2014). ShallowFlow: A Program to Model Ship Hydrodynamics in Shallow Water, *Proceedings of the ASME 33rd International Conference on Ocean, Offshore and Arctic Engineering, OMAE 2014*, San Francisco, California, USA.
14. Vantorre, M.; Journée, J. M. J. (2003). Validation of the strip theory code SEAWAY by model tests in very shallow water, *Numerical Modelling Colloquium*, Flanders Hydraulics Research, Antwerp, October 2003. DUT-SHL Report Nr. 1373-E.
15. Gourlay, T.P.; von Graefe, A.; Shigunov, V.; Lataire, E. (2015). Comparison of AQWA, GL RANKINE, MOSES, OCTOPUS, PDSTRIP and WAMIT with model test results for cargo ship wave-induced motions in shallow water, *Proceedings of the ASME 34th International Conference on Ocean, Offshore and Arctic Engineering, OMAE 2015*, St. John's, Newfoundland, Canada.
16. Gourlay, T.P. (2011). A brief history of mathematical ship-squat prediction, focussing on the contributions of E.O. Tuck, *Journal of Engineering Mathematics* 70: pp. 5-16. doi 10.1007/s10665-010-9435-3.
17. Gourlay, T.P.; Lataire, E.; Delefortrie, G. (2016). Application of potential flow theory to ship squat in different canal widths. To be submitted to *4th International Conference on Ship Manoeuvring in Shallow and Confined Water, MASHCON 2016*, Hamburg, Germany.
18. Gourlay, T.P. (2013). Duisburg Test Case containership squat prediction using ShallowFlow software, *Proceedings of PreSquat Workshop on Numerical Ship Squat Prediction*, Duisburg, Germany.
19. Trimble. (2012). *Trimble R10 GNSS receiver User Guide: Chapter 5 Specifications* (Revision A). California, USA.
20. Gourlay, T.P.; Ha, J.H.; Mucha, P.; Uliczka, K. (2015). Sinkage and trim of modern container ships in shallow water. *Proceedings of the Coasts & Ports 2015 Conference*, Auckland, New Zealand.

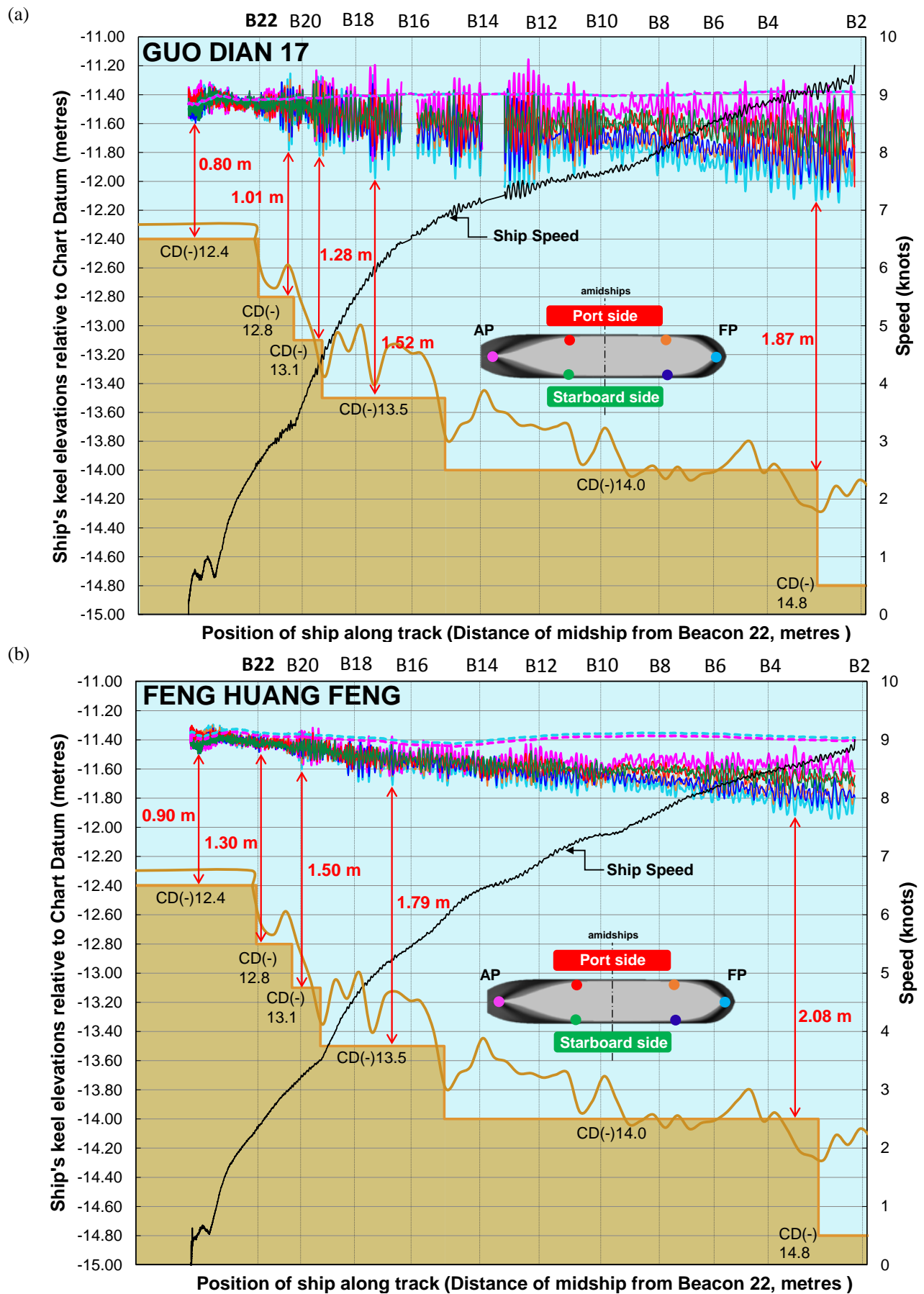
9 AUTHORS BIOGRAPHY

Jeong Hun Ha is a Ph.D. candidate at the Centre for Marine Science and Technology (CMST) at Curtin University, Australia. His Ph.D. thesis is about ship under-keel clearance in port approach channels. His background is as a Korean civil engineer in the design of port and coastal structures.

Tim Gourlay is a Senior Research Fellow at CMST and is supervising Jeong Hun Ha's Ph.D. thesis. He undertakes research and consulting work in ship under-keel clearance for ports in Australia and internationally. He is the author of ShallowFlow software, and has conducted full-scale ship motion measurements on 42 cargo ships and numerous smaller vessels.

Nandakumaran Nadarajah is a Research Fellow at the GNSS Research Centre at Curtin University, Australia. His main areas of interest are signal processing, target tracking, and relative navigation and attitude determination.

APPENDIX



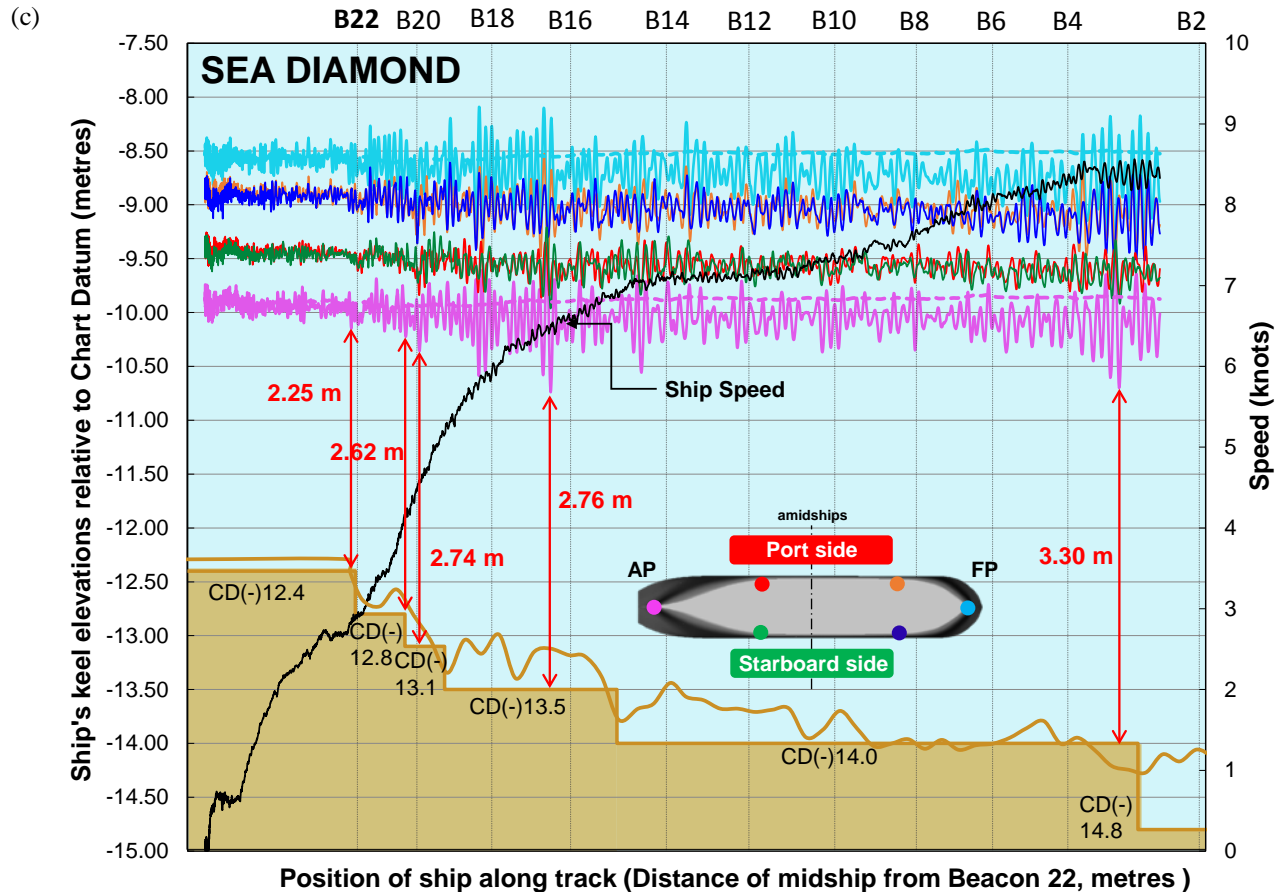


Figure 11. Elevation of the ship's keel relative to chart datum for (a) GUO DIAN 17, (b) FENG HUANG FENG and (c) SEA DIAMOND. Broken lines are elevations of the FP and AP including changes in tide only, i.e. their static position, not including squat and wave-induced motions. A flat seabed line is based on the charted depth on AUS 81, and a fluctuating seabed line is the actual survey line provided by OMC International.